

DEVELOPMENT OF AN ANALYSIS OF A  
REGENERATIVE PUMP

by

JOHN ALBERT OELRICH

B.S.M.E. and B.S.I.E., Washington University

(1949)

M.S.M.E., Newark College of Engineering

(1952)

SUBMITTED IN PARTIAL FULFILLMENT

OF THE REQUIREMENTS FOR THE  
DEGREE OF MECHANICAL ENGINEER

at the

MASSACHUSETTS INSTITUTE OF  
TECHNOLOGY

August 24, 1953

Signature of Author . . . . .  
Department of Mechanical Engineering  
August 24, 1953

Certified by . . . . .  
Thesis Advisor

Accepted by . . . . .  
Chairman, Departmental Committee on  
Graduate Students

DEVELOPMENT OF AN ANALYSIS OF A REGENERATIVE PUMP  
by John A. Oelrich

Submitted to the Department of Mechanical Engineering on August 24, 1953 in partial fulfillment of the requirements for the degree of Mechanical Engineer.

Development of the regenerative pump, although it is industrially attractive because of its unique operational features and design, has trailed far behind that of other hydrodynamic units. This is mainly so because a suitable analytical theory has not been available to predict and improve performance.

This thesis presents a theory and equations satisfying details of the experimentally observed performance. A hypothesis of operation is stated, and a frictionless "ideal" model analyzed. It is shown that the equations for such a model without irreversibilities are incompatible with the known mechanics. Without abandoning the original assumptions, the idealization is then modified to include friction in the differential equations of motion. However, this is shown to complicate the mathematics unreasonably. These analytical difficulties are circumvented using the equations previously derived for the "ideal" model in conjunction with a theory for the effect of shear on the tangential velocity profile and a theory on the form of the losses. The remarkable agreement between the theoretical solution and the experimental data is demonstrated for the pump used in the tests for air at 3600 rpm, and for both air and water on a dimensionless basis.

The analysis is more complete than that for other turbomachinery in that the theoretical solution defines the complete range of operation. It is unusual since only three independent constants, uninfluenced by speed or fluid medium, are introduced. Correlation of the theory and experiment shows that the three constants, solved for simultaneously from data of only the head-capacity curve, result in theoretical equations defining the efficiency and horsepower curves as well as the head curve to equal accuracy.

A program is outlined for further analytical and experimental study of the regenerative pump.

Thesis Supervisor:

W. A. Wilson

Title: Associate Professor of  
Mechanical Engineering

TABLE OF CONTENTS

	Page
Abstract . . . . .	11
List of Illustrations . . . . .	iv
List of Symbols . . . . .	vi
Acknowledgements . . . . .	viii
I. Introduction . . . . .	1
II. Hypothesis of Operation . . . . .	8
III. The "Ideal" Model . . . . .	9
IV. Tangential Velocity Equations of the "Ideal" Model. . . . .	17
V. Tangential Pressure Relation of the "Ideal" Model. . . . .	27
VI. Capacity Equation of the "Ideal" Model . . . . .	29
VII. Radial Pressure Rise Through Rotor of "Ideal" Model. . . . .	32
VIII. Radial Pressure Rise in Open Channel of "Ideal" Model . . . . .	36
IX. Circulatory Flow Equation of "Ideal" Model . . . . .	42
X. Efficiency of "Ideal" Model . . . . .	43
XI. Analysis of an "Ideal" Model . . . . .	45
XII. Introduction of Friction in Equations of Motion. . . . .	50
XIII. Analysis of a "Real" Pump . . . . .	51
XIV. Correlation of Theory and Experimental Data . . . . .	57
XV. Summation . . . . .	72
Appendix . . . . .	75
Bibliography . . . . .	81

LIST OF ILLUSTRATIONSFigures

Figure	Page
1 . . . . .	3
2 . . . . .	13
3 . . . . .	13
4 . . . . .	15
5 . . . . .	16
6 . . . . .	18
7 . . . . .	21
8 . . . . .	23
9 . . . . .	25
10 . . . . .	34

Graphs

Graph	Page
1 - Theoretical and Experimental Performance at 3600 rpm of Regenerative Pump . . . . .	60
2 - Regenerative Pump Theoretical Dimensionless Head Coefficient Compared with Air and Water Experiments	61
3 - Regenerative Pump Theoretical Efficiency Compared with Air and Water Experiments . . . . .	62
4 - Regenerative Pump Theoretical Dimensionless Power Coefficient Compared with Air and Water Experiments	63
5 - Internal Performance Parameters at 3600 rpm of Regenerative Pump . . . . .	66
6 - Theoretical Power Distribution at 3600 rpm of Regenerative Pump . . . . .	68

Graphs, cont.

Graph	Page
7 - Calculated Tangential Flow Angles . . . . .	70
8 - Experimental Tangential Flow Angles . . . . .	71

Photograph

Photograph of Rotor and Internal View of Test Pump . .	76
--	----

LIST OF SYMBOLS

- $a$  - area, cross sectional, of impeller vane  
 $A$  - area, total cross-sectional, general  
 $b, c, d$  - pump dimensions  
 $C$  - coefficient, general  
 $D$  - diameter  
 $f$  - friction factor  
 $g$  - acceleration, gravitational  
 $H$  - head, total, at a point  
 $TH$  - head, total, across pump  
 $HP$  or  $HP$  - horsepower  
 $J$  - Bessel function  
 $K$  - shear loss coefficient  
 $L, \lambda$  - length, streamline, axial direction  
 $M$  - mass flow per unit time  
 $p$  - pressure per unit area (intensity of)  
 $Q$  - discharge, total fluid, from pump  
 $Q_c$  - circulatory flow, radial, through one side of impeller  
 $r$  - radius, general  
 $r_{cg}$  - radius, to center of gravity of open channel area  
 $R$  - radius, to center of gravity of impeller vane  
 $T$  - torque, about axis  
 $W$  - work  
 $U$  - velocity, of point of runner

List of Symbols, continued

- $v$  - velocity, relative, water to runner  
 $V$  - velocity, absolute  
 $V_r$  - velocity, radial component, absolute  
 $V_u$  - velocity, tangential component, absolute  
 $V_z$  - velocity, axial component, absolute  
 $\sigma$  - ratio of tangential velocity of fluid to impeller velocity at blade root, point 1 -  $V_{u1}/U_1$ .  
 $\beta$  - flow angle, tangential, between perpendicular to radius and stream line, in radial plane  
 $\Delta$  - change in any property between two points  
 $\eta$  - efficiency  
 $\theta$  - angle, measured from pump inlet, about axis  
 $\rho$  - density, mass per unit volume  
 $\sigma$  - ratio of tangential velocity of fluid to impeller velocity at periphery of rotor, point 2 -  $V_{u2}/U_2$ .  
 $\phi = \frac{\Phi}{\omega}$  - ratio of tangential pressure gradient to circulatory flow  
 $\omega$  - velocity, angular

ACKNOWLEDGEMENTS

This study is being conducted under a grant contributed to the Massachusetts Institute of Technology by Worthington Corporation, whose interest in the regenerative class unit has extended over many years. Special recognition must go to Mr. R. M. Watson, Worthington's director of research, and Professor W. A. Wilson of the Department of Mechanical Engineering at M.I.T., who conceived and promoted the project. In the interest of furthering the concept of cooperation between industry and educational institutions, Mr. Watson sent a member of Worthington's Research and Development Department (myself) to work at the Institute under the supervision of Professor Wilson.

Acknowledgement is made to Sta-Rite Products, Inc., for the blueprints, test data, and the test unit used in the experiments. I also wish to thank Professors A.H. Shapiro and K. R. Wadleigh for their helpful advice on parts of the analysis.

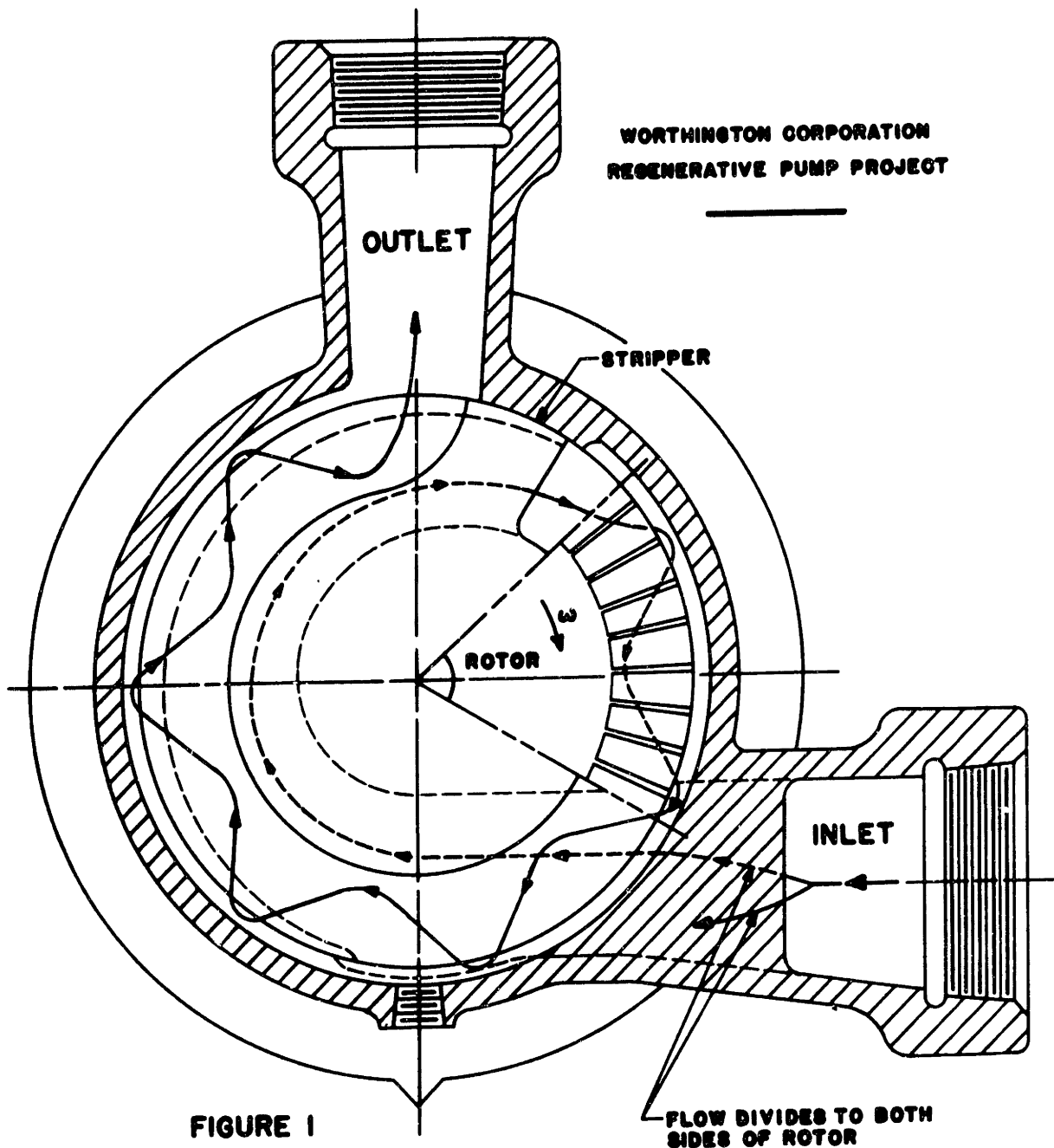


## I. INTRODUCTION

For decades the regenerative pump has excited the interest of inventors, engineers, and manufacturers in Europe, the Far East, and in this country, because of its unique design and operational features. Through the years ingenious inventors and clever engineers have developed the several excellent characteristics of this class of pump by variations in design, often enough very complicated. However, despite the sale of thousands of this type pump throughout the world each year, very little previous investigation of the operating theory has been reported. And those papers which have been submitted far from satisfy the easily determined mechanics. In this thesis is presented a step by step development of equations meeting the experimentally observed performance. First, the equations are derived for an "ideal" model, that is, one restricted to specific assumptions and known facts but without the influence of friction. Friction is then introduced and found to result immediately in complicated Bessel functions not warranted in the light of the previous assumptions. Using the equations for the "ideal" model, the real pump is next approached by the use of two further assumptions, and the close agreement of the theoretical equations for total head, efficiency, and horsepower input demonstrated against experimental data.

Although general recognition may not be conceded, as a class regenerative pumps fall into the vacancy between

rotary positive displacement and low specific speed centrifugal pumps. Fundamentally, the regenerative pump is a hydrodynamic unit obeying the same laws of similitude governing axial flow, mixed flow and centrifugal turbomachinery. In its performance, however, it closely challenges the rotary pump, having a sharply rising head curve, low maximum capacity, and excellent self-priming characteristics. The flow through the type of regenerative unit studied is shown in Figure 1, page 3. In this design the suction divides the fluid to curved, diverging channels leading tangentially into the sides of the impeller. As in other turbomachinery, a free-rotating impeller is utilized. The impeller, in general (see photograph in Appendix), has radial teeth or vanes machined into each side at its periphery which produce a series of helical flows, returning the fluid repeatedly through the vanes for additional energy as it passes through an open annular chamber. It is from this internal multi-staging or regenerative flow pattern, shown for a high capacity in Figure 1, that the pump properly derives its name. Closing the circuit between inlet and discharge is the stripper or septum. Through this region the open channel closes to within a few thousandths of an inch of the sides and tip of the rotor and allows only the fluid then within the impeller to pass through to the suction.



HYDRAULIC AND CONSTRUCTION FEATURES  
OF A REGENERATIVE PUMP

The major characteristic of the regenerative flow pattern is the establishment of extremely large total heads at very low flow rates. This feature, combined with the benefits of rotating machinery construction, makes it very attractive for use in control, filtering, and booster systems, and potentially as a boiler feed pump for marine and other smaller units. Application has been wide and varied in both domestic and industrial installations. Designs have been developed to meet the need where a large pressure rise, high suction-lift, or the ability to handle fluid-vapor mixtures have been of prime importance. Future uses may well be as a compressor and possibly as a turbine.

The name "regenerative pump" has been used religiously so far in this discussion. Historically, the names by which these pumps were and are known are at least as numerous as the ingenious ideas which have been awarded patents. The Spoor Pump and Lupfer Pump took their names from the inventors, as have many others. In England they come under the heading of "Self-Priming Domestic Pumps" of one manufacturer. Further, and more descriptive, names which have been given the regenerative class are "turbine pump," "friction pump," "vortex pump," "self-priming pump," "rotary turbine pump," and, by one enthusiastic manufacturer, the "Magic Wonder Pump."

Disadvantages of the regenerative pump are the relatively low efficiencies obtained, lack of theoretical information to predict and improve performance, and its inability to handle fluids containing solids since abrasion would soon open the extremely small clearances. The side clearance and the radial clearance through the stripper, which are generally of the order of .001 inch to .003 inch, produce a further disadvantage. Excellent workmanship and close quality control become necessary in manufacture and limit mass production possibilities. This fact, coupled with low efficiency, has been the major reason why Europe has made more use of the regenerative class than has the United States.

Theoretical and experimental investigation was begun in the fall of 1952, using as a model the Sta-Rite 1 $\frac{1}{2}$ -TH-7 regenerative pump. At this time a group of four seniors elected the project as their undergraduate thesis. One pair, Daniel A. Lippman and Theodore Taylor, Jr., designed and constructed the test equipment and made certain modifications in the pump. The second pair, Luis R. Lazo and Thomas J. Hopkins, attempted a general theoretical and experimental analysis in conjunction with myself. The work of Lazo and Hopkins will be referred to frequently, particularly in comparison with the theoretical solution. Gilbert F. Lutz, another senior, continued the experimental work in the spring of 1953. As with Lazo and Hopkins,

his work was directed toward an understanding of the operational characteristics of the regenerative pump and the verification of assumptions used in the theoretical analysis. Aiding in the development of the analysis during this period was Miguel A. Santalo, a teaching assistant, who elected to pursue one of the phases of the overall project as his master's thesis.

It became apparent from the first experimental investigations that the few previously reported analyses are not compatible with the present conception of the pump's mechanics. The most complete analysis in the current literature is that of Yasutashi Senoo.<sup>1</sup> In Mr. Senoo's paper the unit is labeled a "friction pump" and turbulent friction between the moving impeller and the fluid is considered the primary force causing the pumping action. The flow is assumed to be two-dimensional in cylindrical planes about the pump axis, which are straightened for simplicity. The velocity profile is further assumed not to vary between blade root and tip. For this turbulent process Mr. Senoo applies Prandtl's mixing length theory, estimating the turbulent viscosity. This analysis may, in part, explain the mechanism in the

---

<sup>1</sup> "Theoretical Research on Friction Pump," Reports of the Research Institute for Fluid Engineering, Vol.5, No.1, Japan, 1948.

radial area of the open channel. However, it completely ignores the more fundamental circulatory motion imposed by the centrifugal field and so gives no information on the mechanics of motion as a hydrodynamic unit.

A second paper, written by Warren E. Wilson,<sup>1</sup> director of research of the Sundstrand Machine Tool Company, again points to the fact that theoretical investigation of the regenerative class has not been based on its own merits, even though the principal operating characteristics were noted by the first inventors. In agreement with a Japanese investigator, A. Mizadzu,<sup>2</sup> Mr. Wilson classifies the "turbine pump" as a rotary pump, asserting that "this classification is sound since the theory of operation of the rotary pump is adequate to account for the performance characteristics." Mr. Wilson then analyzes the regenerative pump in a fashion similar to a hydrodynamic bearing, assuming only the radial area of the open channel to be worthy of note.

Such has been the scanty investigation of the regenerative pump. The author and his colleagues believe that in this paper a closer approach to the true nature of the complicated mechanics of the regenerative pump is offered.

---

<sup>1</sup> "Analysis of Turbine Pumps," Product Engineering, October, 1947.

<sup>2</sup> "Theory of Wesco Rotary Pump," Transactions of the Society of Mechanical Engineers of Japan, Vol.15, No.18, February, 1939.

## II. HYPOTHESIS OF OPERATION

The following paragraphs describe a hypothesized mechanism of the internal functioning of the pump. This mechanism is described in terms of a circulatory or meridional flow,  $Q_c$ , superposed on a tangential or through flow,  $Q$ . It is assumed that these two flows are independent of circumferential position in the working section of the pump.

As the circulatory flow passes radially through the rotor its angular momentum in the direction of rotor motion is materially increased by the work of the impeller. In order to maintain a tangential pressure gradient, the angular momentum of the circulatory flow as it traverses the stream path in the open channel must continually decrease from its original value on leaving the rotor to provide the necessary impulse. Therefore, as we follow the circulatory flow along the flow path its tangential velocity component must decrease (or reverse). Qualitatively, this indicates that the sharply rising pressure gradient, experimentally observed as thru-flow is decreased, depends on either an increase in the rate of the circulatory flow or greater reduction of the tangential velocity of the circulatory flow from the exit of the rotor to its entrance, or both.



The net thru-flow or capacity,  $Q_c$ , is the integral over the area of the open channel of the tangential velocity times the associated differential element of area. (Fluid enclosed by the vanes of the rotor when it reaches the stripper is carried through into the pump suction.) Reductions in the tangential velocity outside the rotor result in reductions in capacity. On this basis alone higher pressures may be anticipated at reduced capacity as observed. In addition, however, it can be shown that the circulatory flow varies with decreasing capacity to increase further the tangential pressure gradient. Since the centrifugal field creating the radial pressure gradient inside the rotor is constant, whereas the field due to the external vortex weakens as the tangential velocities decrease, the rate of the circulatory flow may be expected to increase continuously as we approach zero thru-flow.

Experimental results also show that power requirements increase with decreasing capacity. Assuming the angular momentum of the fluid leaving the rotor is constant, or nearly so, the hypothesis of operation stated satisfies this condition since the change in angular momentum per unit of circulatory flow which the rotor must produce increases with reduced capacity, and  $Q_c$  is simultaneously increasing.

### III. THE "IDEAL" MODEL

The actual three-dimensional character of the fluid motion within the regenerative pump can be described only

generally in qualitative statements. The working equations from the solution of the differential equations of motion for the three-dimensional case of this complex flow, assuming they could be obtained, would be so extremely complicated as to make them of doubtful value for use as an engineering solution. We therefore introduce the concept of an "ideal" model similar in principle to those used elsewhere in the field of fluid mechanics and other fields. The selection of a representative stream line, the use of one- or two-dimensional flow, and the assumption of velocity diagrams unaffected by friction are common in the study of turbines, compressors, and pumps.

One underlying purpose in assuming an "ideal" model is the development of a standard for the ultimate performance of the regenerative pump. In Section XI it is shown that the assumption of a linear pressure gradient tangentially which is consistent with the known mechanics of the actual unit, and which must then be applicable to a "true" model, is not compatible with the assumption of frictionless processes in an "ideal" regenerative pump. It is deduced there that irreversibilities must be considered in order to obtain a solution compatible with the known performance. The question legitimately arises as to the usefulness of the detailed analysis of the "ideal" frictionless model, which immediately follows this section, if performance characteristics of the fully "ideal" pump

cannot be obtained. Again referring to later sections of this thesis, it is demonstrated that the introduction of friction directly in the differential equations of motion results in extreme mathematical complications. The answer to the question of the usefulness of the analysis without friction is that these complications are circumvented by a modification of the idealization which allows the inclusion of irreversibilities in simple terms in the equations derived for the "ideal" model.

In our study of the "ideal" regenerative pump we assume that -

- a) fluid shear is negligible;
- b) flow is steady and fluid incompressible;
- c) there is no internal leakage;
- d) all processes within the pump are adiabatic;
- e) characteristic flow is one-dimensional in each major direction (radial, tangential, and axial);
- f) there are no end effects due to suction, discharge, and stripper.

From experiments by Lazo and Hopkins and by Lutz, we also have the facts that the -

- g) tangential pressure gradient is independent of radius;
- h) tangential pressure gradient about the periphery is linear;

1) unit is governed by the same laws of similitude as other fluid dynamic apparatus.

Figure 2 on page 13 illustrates that the assumption of one-dimensionality reduces the flow to a mean stream surface circling a hypothetical barrier. Actually, extensive experiments show that fluid leaves or enters the rotor along the entire radial length of the vane, and the radius beyond which there is a net outflow changes with capacity. We define a mean stream line on the stream surface as the path of the average tangential and radial (or axial) velocities of the absolute motion. That is, the circulatory flow following a meridional projection of a mean stream line has, point by point along the flow path projection, the tangential velocity of the thru-flow. A mean stream line is shown through the working section of the pump in Figure 1, page 3, and again in Figure 4 a), page 15.

Since pressure measurements taken about the periphery of a test pump have shown that the tangential pressure gradient is essentially linear, the analysis of any meridional section of the working portion of the pump will give the equations of motion characteristic of the entire unit. We therefore select for analysis an arbitrary element  $d\theta$  of the working section of the pump.\* We further subdivide

---

\* This analysis applies to a single flow pump whereas commercial units are characteristically double flow, i.e., consist of two single flow units back to back.

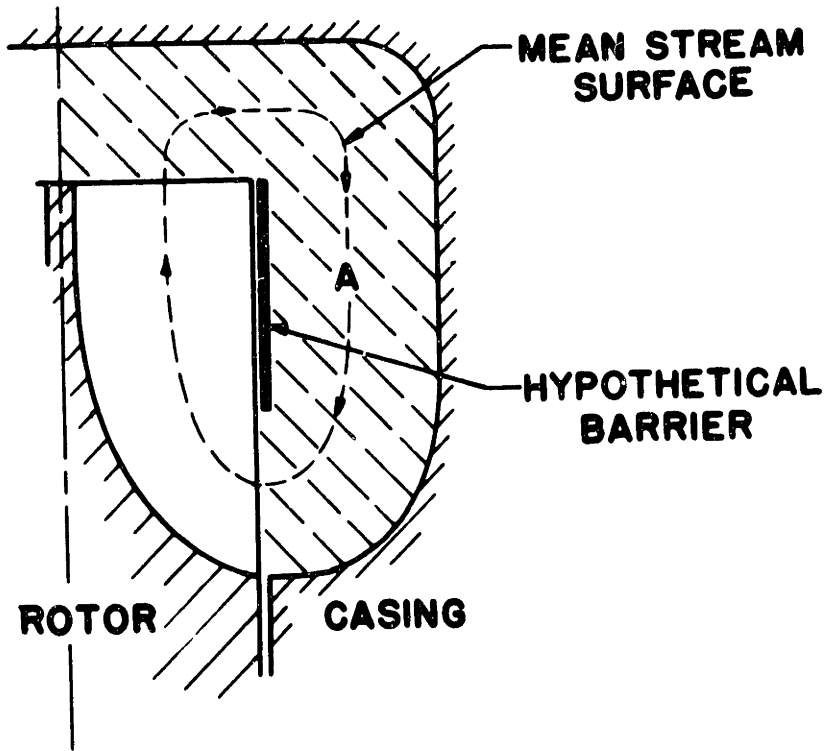


FIGURE 2

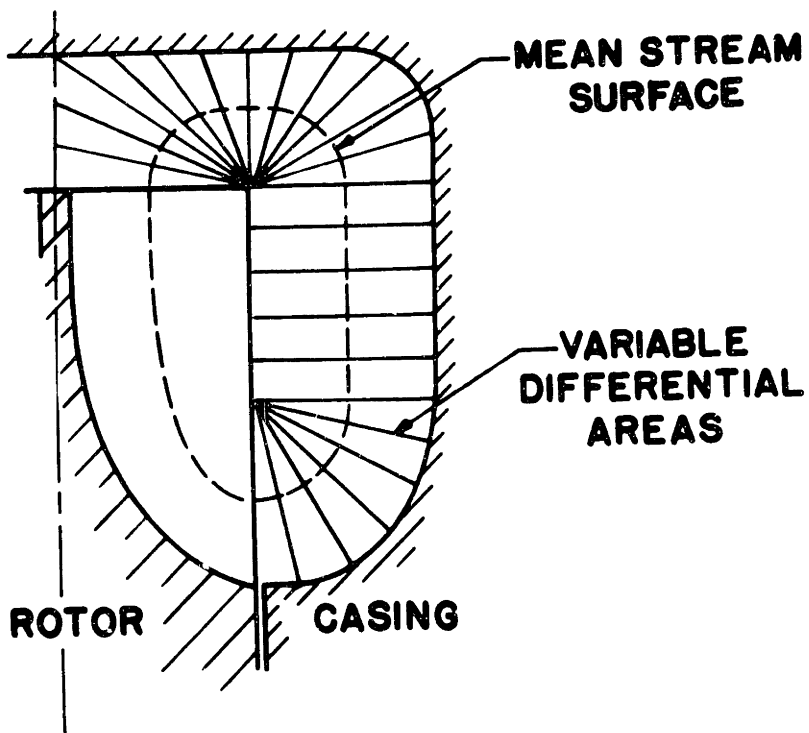


FIGURE 3

the open channel volume included in this element into four subdivisions for each of which the differential equations can be set up by considering a typical differential control volume. Typical meridional surfaces of the differential control volumes are shown in Figure 4 b) on page 15. The control volumes have differential extent in the meridional and tangential directions, such as  $dr$  and  $r d\theta$  or  $dz$  and  $r d\theta$ , and a finite meridional width which must be based on the local dimension normal to the circulatory flow path, such as  $d$  in the main section of the open channel. To avoid analytic complication, the projection of the meridional mean stream surface is taken as rectilinear as shown in Figure 4 b) rather than curvilinear as in Figures 2 and 3. The kind of complication which would ensue from the latter choice is apparent in Figure 3.

The consequence of the assumption actually made is that two flow patterns are actually attributed to single meridional areas  $m$ ,  $n$ , and  $o$  as shown in Figure 5, page 16, whereas the areas  $w$ ,  $x$ , and  $y$  have no flows assigned to them. It has been assumed that the dual inclusion of the former areas very nearly compensates for the exclusion of the latter. The propriety of the assumption may be adjudged from the fact that each of the small areas in question is approximately 0.01 square inches as compared to the total meridional cross section of the pump of 0.75 square inches for the test model.

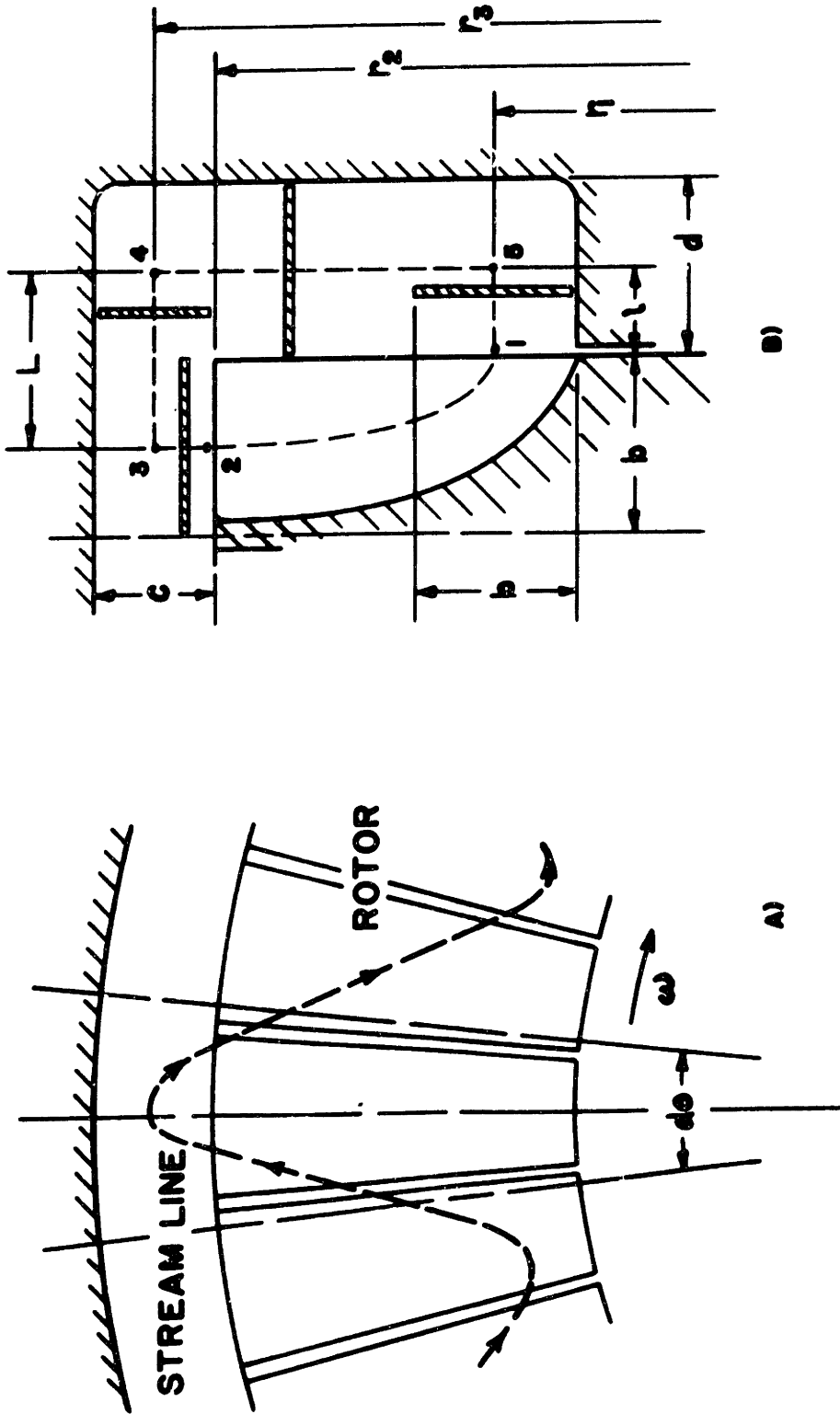


FIGURE 4

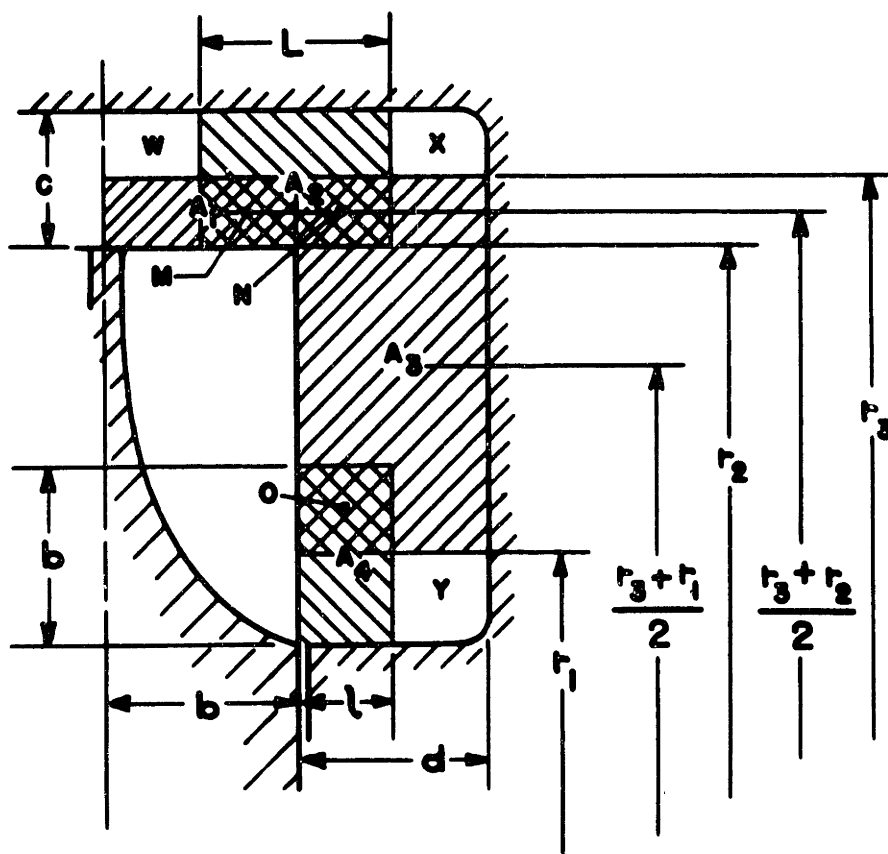


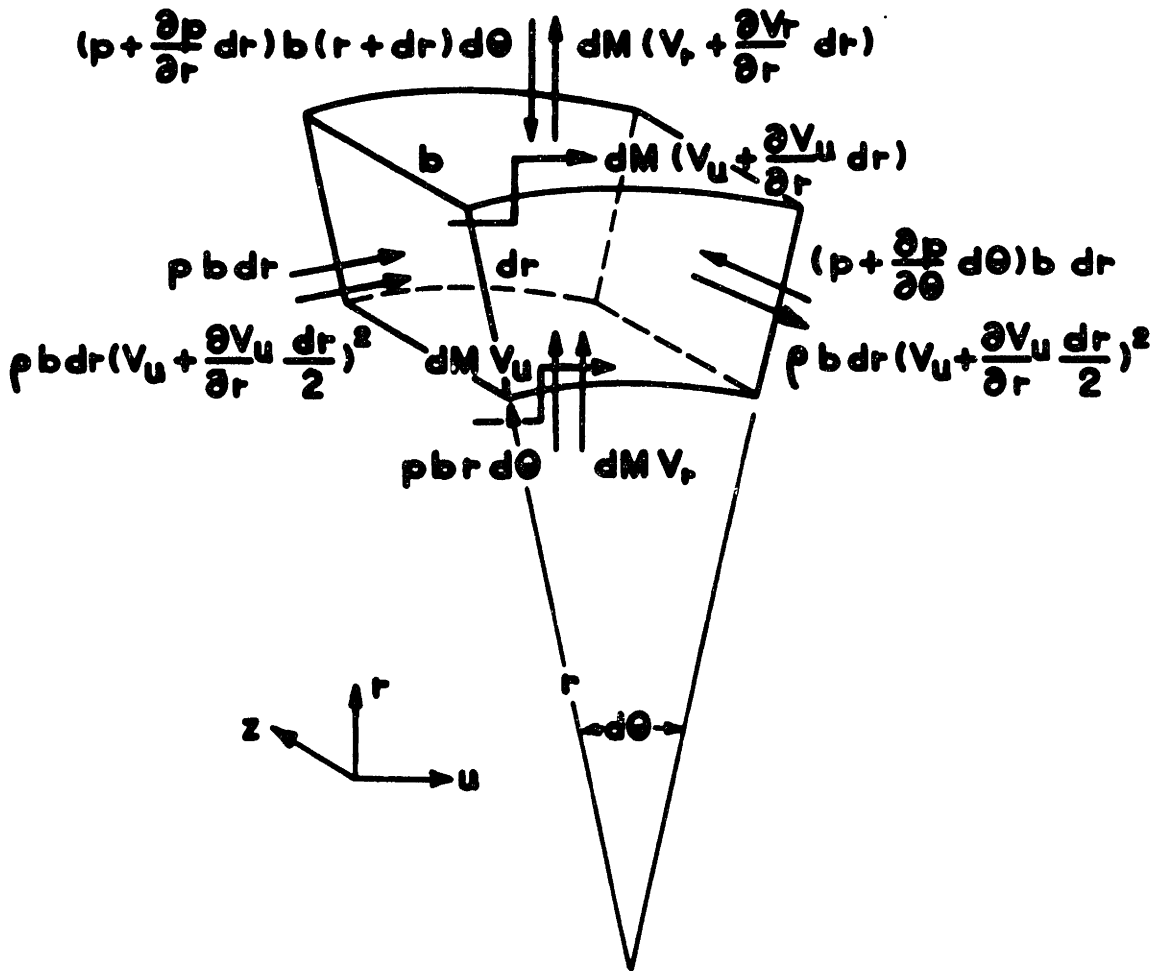
FIGURE 5



#### IV. TANGENTIAL VELOCITY EQUATIONS OF THE "IDEAL" MODEL

To satisfy the condition of identical mechanics throughout the working section of the pump, the absolute fluid velocity must be independent of circumferential position. Accelerations in the tangential velocity between two similar meridional points are therefore excluded and the mass rate of the tangential flow through all corresponding meridional areas is constant. Consider a typical differential control volume within an arbitrary element of the pump, as described in the last section: since the mass entering and leaving the volume tangentially must be the same, the principle of conservation of mass or continuity demands that the mass rate of the circulatory flow,  $dM$ , through the volume must be independent of the position radially or axially.

The differential equations of the tangential motion are obtained by applying Newton's second law, formulated for angular momentum, to a differential control volume of each of the previously defined subdivisions of a meridional element. We will first investigate the control volume  $b \, dr \, d\theta$  between points 2 and 3 of the meridional projection of a mean stream line (see Figure 4, page 15, and Figure 6, page 18), using only those forces pertaining to the tangential motion. Since as we move radially outward in the direction of the circulatory flow the angular momentum must decrease to support a positive pressure gradient, Newton's second law gives us:



**CONTROL VOLUME BETWEEN POINTS 2 & 3**

**FIGURE 6**

$$p b dr \left( r + \frac{dr}{2} \right) - \left( p + \frac{\partial p}{\partial \theta} d\theta \right) b dr \left( r + \frac{dr}{2} \right) =$$

$$dM \left( V_u + \frac{\partial V_u}{\partial r} dr \right) (r + dr) - dM V_u r$$

Performing the indicated operations and neglecting quantities small to the second order reduces this equation to:

$$\frac{\partial V_u}{\partial r} + \frac{V_u}{r} = - \frac{\partial p}{\partial \theta} \frac{d\theta}{dM} b$$

a differential equation for  $V_u$  (the tangential velocity) as a function of the radius,  $r$ , since by assumption and experimentation the tangential pressure gradient, as well as the mass rate of the circulatory flow,  $dM$ , is independent of radius. It is interesting to note that if the tangential pressure gradient is zero the solution of this differential equation gives the relation for a free or potential vortex,  $V r = \text{constant}$ .

Before solving this equation we introduce at this point the concept of the "coefficient of slip" similar to the Busemann factor<sup>1</sup> or Stodola correction<sup>1</sup> for runner head used in centrifugal pumps. These investigators assumed a fluid motion through centrifugal pump impellers uninfluenced by stationary guide-vane systems or casing. Under this assumption, which eliminates the otherwise unsteady character

---

<sup>1</sup> See Chapter 10, paragraph 53, Fluid Mechanics of Turbomachinery, by George F. Wislicenus, McGraw-Hill, New York, 1947.

of the absolute motion, the tangential velocity at the rotor periphery of radial-flow impellers was determined to be dependent only on the design; that is, number, length, spacing, and angle of the vanes. For impellers with a vane length equal to or greater than the spacing at the periphery, the work of both Busemann and Stodola indicates that the velocity correction is independent of capacity. The "coefficient of slip", which we will call  $\sigma$ , and which will be assumed constant, relates the actual tangential velocity of the fluid leaving the impeller,  $V_{u2}$ , to the tip speed of the rotor,  $U_2$ :

$$V_{u2} = \sigma U_2 \quad (1)$$

For future convenience in the derivations we also define,

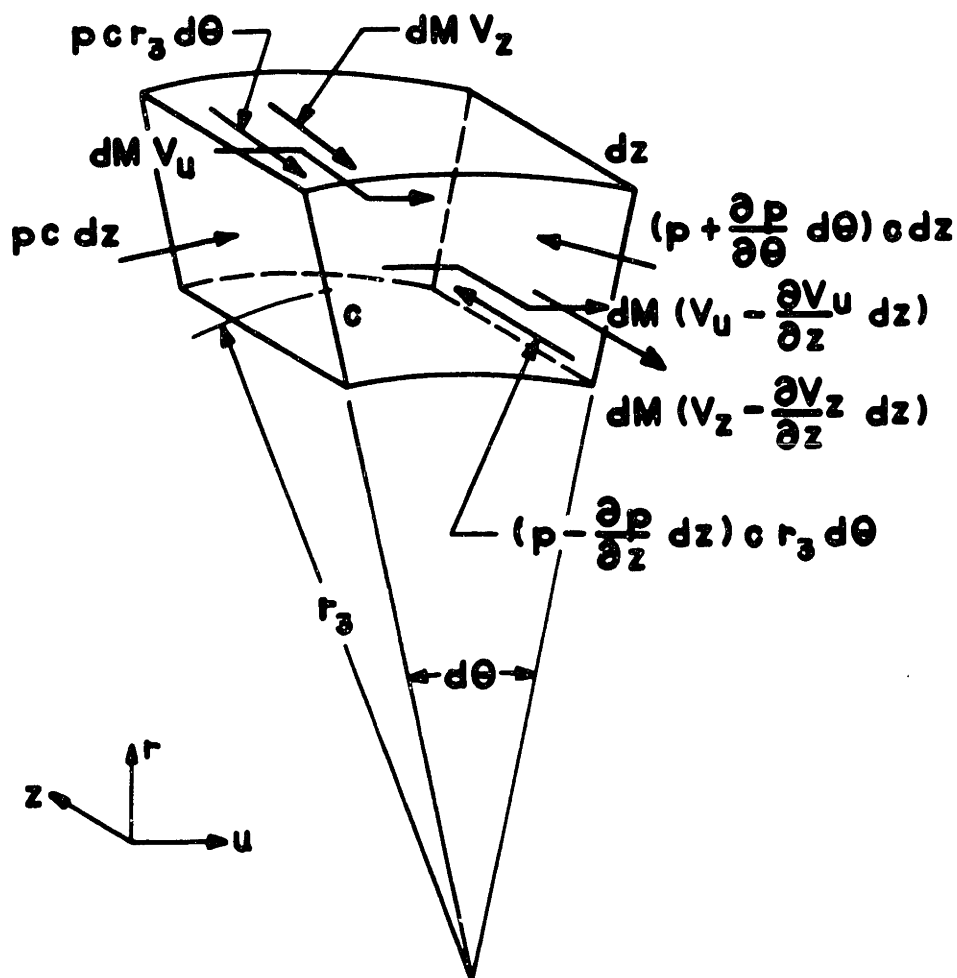
$$\frac{\partial p}{\partial \theta} \frac{d\theta}{dM} = \phi \quad (2)$$

Solving the above differential equation with the condition that  $V_{u2} = \sigma U_2$  when  $r = r_2$ ,

$$V_{u(s-s)} = \frac{r_2}{r} \sigma U_2 - \phi \frac{b}{2} \left[ \frac{r^2 - r_2^2}{r} \right] \quad (3)$$

a function for the tangential velocity between points 2 and 3.

In accordance with our one-dimensional assumptions, the tangential velocity does not vary with radius from point 3 to point 4 along the meridional projection of a mean stream line, but decreases as we move in the axial,  $z$ , direction. For the element  $c \, dz \, d\theta$ , shown in Figure 7,



CONTROL VOLUME BETWEEN POINTS 3 &amp; 4

FIGURE 7

page 21, angular momentum in the tangential direction gives us,

$$p c r_s dz - \left( p + \frac{\partial p}{\partial \theta} d\theta \right) c r_s dz = dM \left( V_u - \frac{\partial V_u}{\partial z} dz \right) r_s - dM V_u r_s$$

from which we determine,

$$dV_u = \frac{\partial p}{\partial \theta} \frac{d\theta}{dM} c dz$$

Noting that the pressure gradient and  $dM$  are also independent of  $z$  and that  $V_u = V_{us}$  at point 3, that is, when  $z = z_s$ , we integrate:

$$\int_{V_{us}}^{V_u} dV_u = \phi c \int_{z_s}^z dz$$

$$V_u = V_{us} - \phi c (z_s - z)$$

The velocity  $V_{us}$  is determined from equation (3)

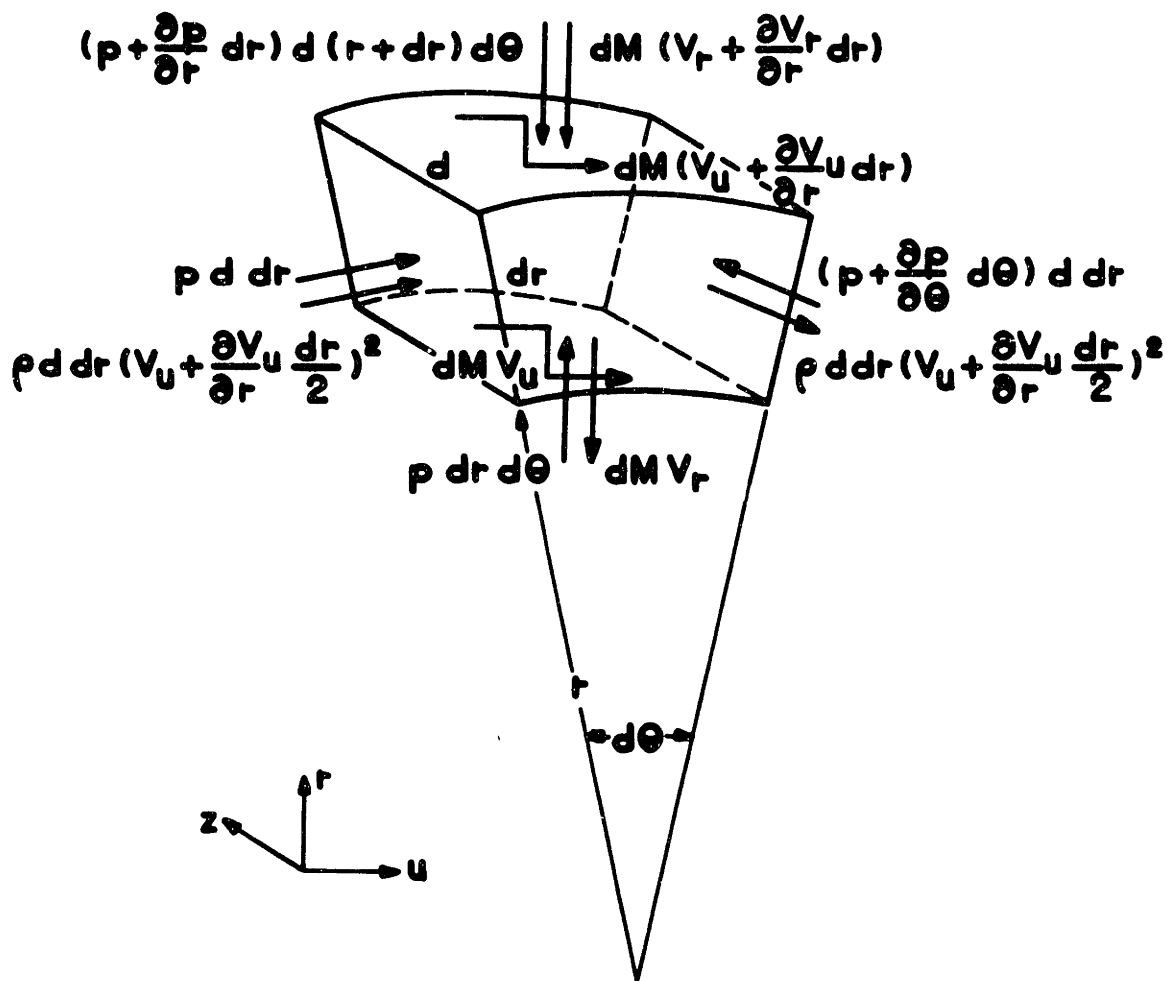
when  $r = r_s$ ,

$$V_{us} = \frac{r_s}{r_s} \sigma U_s - \phi \left[ \frac{b (r_s^2 - r_s^2)}{2r_s} \right]$$

Substituting in the relation above,

$$V_{u(s-4)} = \frac{r_s}{r_s} \sigma U_s - \phi \left[ \frac{b (r_s^2 - r_s^2)}{2r_s} + c (z_s - z) \right] \quad (4)$$

The angular momentum must again decrease as we move radially inward in the direction of the circulatory flow along the projection of a mean stream line from point 4 to point 5 to support a positive pressure gradient. Applied to the differential volume  $d r d\theta$  of Figure 8, page 23, Newton's second law in terms of angular momentum



**CONTROL VOLUME BETWEEN POINTS 4 & 5**

**FIGURE 8**

gives us the relation:

$$p \, d \, dr \left( r + \frac{dr}{2} \right) - \left( p + \frac{\partial p}{\partial \theta} d\theta \right) d \, dr \left( r + \frac{dr}{2} \right) =$$

$$dM \, V_u \, r - dM \left( V_u + \frac{\partial V_u}{\partial r} dr \right) (r + dr)$$

Again neglecting quantities small to the second order, this relation reduces to,

$$\frac{\partial V_u}{\partial r} + \frac{V_u}{r} = \frac{\partial p}{\partial \theta} \frac{d\theta}{dM} d$$

To determine the constant of integration in solving this differential equation we use the end condition,

$$V_u = V_{u4} \text{ when } r = r_s$$

which gives us,

$$V_u = \frac{r_s}{r} V_{u4} - \phi \frac{d}{2} \left[ \frac{r_s^2 - r^2}{r} \right]$$

For the velocity  $V_{u4}$  we turn to equation (4). From Figure 4 b) the length  $(z_3 - z_4)$  from point 3 to point 4 is denoted by  $L$ , so that the tangential velocity at point 4 becomes,

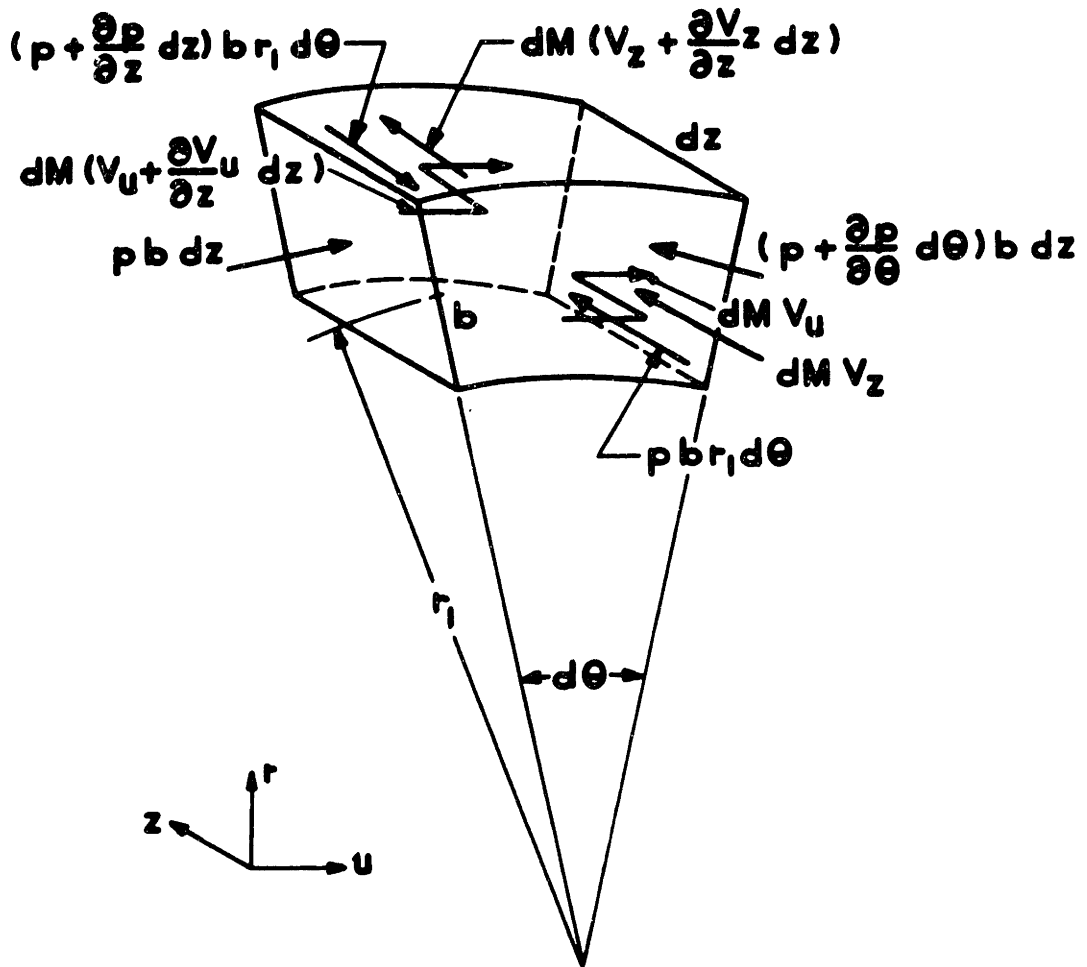
$$V_{u4} = \frac{r_s}{r_s} \sigma U_s - \phi \left[ \frac{b (r_s^2 - r_s^2)}{2r_s} + c L \right]$$

Substituting in the previous equation,

$$V_{u(4-5)} = \frac{r_s}{r} \sigma U_2 - \phi \left[ \frac{b(r_s^2 - r_s^2)}{2r} + \frac{c L r_s}{r} + \frac{d(r_s^2 - r_s^2)}{2r} \right] \quad (5)$$

Along the last segment of the projection of a mean stream line in the meridional plane, from point 5 to point 1, we again assume the tangential velocity varies only in





CONTROL VOLUME BETWEEN POINTS 5 & 1

FIGURE 9

the direction of the circulatory flow, in this case decreasing as we move axially toward the rotor. If we further assume the circulatory flow enters the rotor at point 1 over a radial height equal to the maximum blade width,  $b$ , the tangential impulse-momentum relation for the control volume  $b \, dz \, d\theta$  in Figure 9, page 25, becomes,

$$p \, b \, r_1 \, dz - (p + \frac{\partial p}{\partial \theta} \, d\theta) \, b \, r_1 \, dz = dM(V_u + \frac{\partial V_u}{\partial z} \, dz)r_1 - dM \, V_u \, r_1$$

which reduces to,

$$dV_u = - \frac{\partial p}{\partial \theta} \frac{d\theta}{dM} \, b \, dz$$

At point 5,  $z = z_5$  and  $V_u = V_{u5}$ , which can be determined from equation (5). With this condition for our lower limits,

$$\int_{V_{u5}}^{V_u} dV_u = - \phi \, b \int_{z_5}^z dz$$

$$V_u = V_{u5} - \phi \, b(z - z_5)$$

From equation (5),

$$V_{u5} = \frac{r_2}{r_1} \sigma U_2 - \phi \left[ \frac{b(r_2^2 - r_1^2)}{2r_1} + \frac{c \, L \, r_2}{r_1} + \frac{d(r_2^2 - r_1^2)}{2r_1} \right]$$

so that substitution in the equation above gives us,

$$V_{u(5-1)} = \frac{r_2}{r_1} \sigma U_2 - \phi \left[ \frac{b(r_2^2 - r_1^2)}{2r_1} + \frac{c \, L \, r_2}{r_1} + \frac{d(r_2^2 - r_1^2)}{2r_1} + b(z - z_5) \right] \quad (6)$$

The four equations (3) through (6) give us the thru-flow velocity profile of the "ideal" model along the separate segments of the projection of a mean stream line on the meridional plane. Before using the velocity relations themselves, we note that if the tangential velocity at point 1 is defined, equation (6) can be solved for

$$\phi = \frac{\partial p}{\partial \theta} \frac{d\theta}{dM}$$

#### V. TANGENTIAL PRESSURE RELATION OF THE "IDEAL" MODEL

In the last section the tangential fluid and rotor velocities at the impeller periphery were related by the coefficient  $\sigma$ . This factor was assumed a constant dependent primarily on rotor design. At the blade entrance, point 1, we introduce a strong and useful variable into our development as the coefficient relating the tangential velocity of the fluid to the velocity of the impeller:

$$V_{u1} = \alpha U_1 \quad (7)$$

Unlike  $\sigma$ , the coefficient  $\alpha$  (alpha) must be dependent on the point of operation on the head-capacity curve because of the variation in the velocity profile as operating conditions are changed.

Denoting the length,  $(z_1 - z_5)$ , between point 5 and point 1 by  $l$  (see Figure 4 b), page 15), from equation (6),

$$V_{u_1} = \alpha C U_1 = \frac{r_2}{r_1} \sigma U_2 - \frac{\partial p}{\partial \theta} \frac{d\theta}{dM} \left[ \frac{b(r_2^2 - r_1^2)}{2r_1} + \frac{c L r_2}{r_1} + \frac{d(r_2^2 - r_1^2)}{2r_1} + b \right]$$

Solving for the tangential pressure gradient,

$$\frac{\partial p}{\partial \theta} d\theta = \frac{dM(r_2 \sigma U_2 - r_1 \alpha C U_1)}{\frac{b(r_2^2 - r_1^2)}{2} + c L r_2 + \frac{d(r_2^2 - r_1^2)}{2} + b} r_1$$

This equation may first be simplified by substituting for the dimensions in the denominator the areas  $A_1$  to  $A_4$  referred to in Figure 5, page 16.

$$\frac{\partial p}{\partial \theta} d\theta = \frac{dM(r_2 \sigma U_2 - r_1 \alpha C U_1)}{A_1 \frac{r_2 + r_1}{2} + A_2 r_2 + A_3 \frac{r_2 + r_1}{2} + A_4 r_1}$$

Further comparison with Figure 5 discloses that the denominator is the sum of the first moments of these areas about the pump axis. That this is a natural result may be reasoned from our stipulation, based on experiment, that the tangential pressure gradient is independent of radius. As a consequence of this fact the differential external torque,  $dT$ , acting on the fluid between two surfaces of the open channel, may be written as,

$$dT = \left( \frac{\partial p}{\partial \theta} d\theta \right) r_{cg} A - dM(r_2 \sigma U_2 - r_1 \alpha C U_1)$$

where  $r_{cg}$  is the radius to the center of gravity of the area  $A$  of one-half the pump. Through the working section of the "ideal" pump, however, the external torque is zero

on the boundaries (casing) of the open channel. This reduces the tangential pressure gradient relation to:

$$\frac{dp}{d\theta} d\theta = \frac{dM(r_2 \sigma U_2 - r_1 \sigma U_1)}{r_{cg} A} \quad (8)$$

As this is a hydrodynamic unit, we are interested in the total head developed and volume rate of flow of any fluid pumped, not the pressure rise and mass rate of a particular medium. We define as the volume rate of the circulatory flow:

$$Q_c = \frac{dM}{\rho d\theta} \quad (9)$$

With this substitution, and considering the change in head over the angle,  $\theta$ , of the working section of the pump, the theoretical total head developed by the "ideal" model becomes:

$$\Delta H_{tang} = \frac{Q_c (r_2 \sigma U_2 - r_1 \sigma U_1)}{r_{cg} A} \quad (10)$$

where  $Q_c$  is the radial or circulatory flow of half the pump.

## VI. CAPACITY EQUATION OF THE "IDEAL" MODEL

The capacity or thru-flow,  $Q$ , is equal to:

$$Q = \int_A v_u dA$$

Equations for the tangential velocity were derived for each segment of the projection of the mean stream line

on the meridional plane, so rather than a single operation individual integrations are performed along each section.

$$Q = \int_{r_2}^{r_3} V_{u(s-3)} b \, dr + \int_{z_4}^{z_3} V_{u(s-4)} c \, dz + \\ + \int_{r_1}^{r_2} V_{u(4-5)} d \, dr + \int_{z_5}^{z_1} V_{u(5-1)} b \, dz$$

As in the previous section, the areas  $A_1$  to  $A_4$  are substituted as their dimensions occur.

Between points 2 and 3, using equation (3) from page 20,

$$Q(s-3) = \int_{r_2}^{r_3} V_{u(s-3)} b \, dr$$

$$Q(s-3) = r_3 b \sigma U_s \int_{r_2}^{r_3} \frac{dr}{r} - \frac{\phi b^2}{2} \int_{r_2}^{r_3} r \, dr + \frac{\phi b^2 r_3^2}{2} \int_{r_2}^{r_3} \frac{dr}{r}$$

$$Q(s-3) = r_3 b \sigma U_s \ln \frac{r_3}{r_2} + \phi \left[ \frac{b^2 r_3^2}{2} \ln \frac{r_3}{r_2} - \frac{A_1 b (r_3 + r_2)}{4} \right] \quad (11)$$

Between points 3 and 4, using equation (4) from page 22,

$$Q(s-4) = \int_{z_4}^{z_3} V_{u(s-4)} c \, dz$$

$$Q(s-4) = \frac{r_3 c \sigma U_s}{r_3} \int_{z_4}^{z_3} dz - \frac{\phi A_1 c (r_3 + r_2)}{2 r_3} \int_{z_4}^{z_3} dz - \\ - \phi c^2 \int_{z_4}^{z_3} (z_3 - z) dz$$

$$Q_{(s-4)} = \frac{r_2 A_2 \sigma U_s}{r_2} - \phi \left[ \frac{A_1 A_2 (r_2 + r_1)}{2r_2} + \frac{A_2^2}{2} \right] \quad (12)$$

Between points 4 and 5, using equation (5) from page 24,

$$Q_{(4-5)} = \int_{r_1}^{r_2} V_{u(4-5)} d r$$

$$Q_{(4-5)} = r_2 d \sigma U_s \int_{r_1}^{r_2} \frac{d r}{r} - \frac{\phi A_1 d (r_2 + r_1)}{2} \int_{r_1}^{r_2} \frac{d r}{r} -$$

$$- \phi A_2 d r_2 \int_{r_1}^{r_2} \frac{d r}{r} - \frac{d^2 r_2^2}{2} \int_{r_1}^{r_2} \frac{d r}{r} + \frac{d^2}{2} \int_{r_1}^{r_2} r d r$$

$$Q_{(4-5)} = r_2 d \sigma U_s \ln \frac{r_2}{r_1} - \phi \left[ \left( \frac{A_1 d (r_2 + r_1)}{2} + A_2 d r_2 + \right. \right. \quad (13)$$

$$\left. \left. + \frac{d^2 r_2^2}{2} \right) \ln \frac{r_2}{r_1} - \frac{A_2 d (r_2 + r_1)}{4} \right]$$

Between points 5 and 1, using equation (6) from page 26,

$$Q_{(5-1)} = \int_{z_5}^{z_1} V_{u(5-1)} b d z$$

$$Q_{(5-1)} = \left[ \frac{r_2 b \sigma U_s}{r_1} - \frac{\phi A_1 b (r_2 + r_1)}{2r_1} - \frac{\phi A_2 b r_2}{r_1} - \right.$$

$$\left. - \frac{\phi A_3 b (r_2 + r_1)}{2r_1} \right] \int_{z_5}^{z_1} d z - \phi b^c \int_{z_5}^{z_1} (z - z_5) d z$$

$$Q_{(5-1)} = \frac{r_2 A_4 \sigma U_s}{r_1} - \phi \left[ \frac{A_1 A_4 (r_2 + r_1)}{2r_1} + \frac{A_2 A_4 r_2}{r_1} + \right. \quad (14)$$

$$\left. + \frac{A_3 A_4 (r_2 + r_1)}{2r_1} + \frac{A_4^2}{2} \right]$$

Summing equations (11), (12), (13) and (14) to obtain the total capacity,

$$\begin{aligned}
 Q = r_2 \sigma U_2 \left[ b \ln \frac{r_3}{r_2} + \frac{A_3}{r_2} + d \ln \frac{r_3}{r_1} + \frac{A_4}{r_1} \right] - \quad (15) \\
 - \phi \left[ \frac{A_1 b (r_3 + r_2)}{4} + \frac{A_1 A_3 (r_3 + r_2)}{2r_2} - \frac{A_3 d (r_3 + r_1)}{4} + \right. \\
 \left. + \frac{A_1 A_4 (r_3 + r_2)}{2r_1} + \frac{A_3 A_4 (r_3 + r_1)}{2r_1} + \frac{A_3^2}{2} + \frac{A_3 A_4 r_3}{r_1} + \frac{A_4^2}{2} - \right. \\
 \left. - \frac{b^2 r_2^2}{2} \ln \frac{r_3}{r_2} + \left( \frac{A_1 d (r_3 + r_2)}{2} + A_3 d r_3 + \frac{d^2 r_3^2}{2} \right) \ln \frac{r_3}{r_1} \right]
 \end{aligned}$$

where, from equations (2) and (8),

$$\phi = \frac{r_2 \sigma U_3 - r_1 \sigma U_1}{r_{cg} A}$$

a very untidy relation.

## VII. RADIAL PRESSURE RISE THROUGH ROTOR OF "IDEAL" MODEL

So far the equations for the theoretical head and capacity have been derived. The total head developed, however, was shown to be a function of the circulatory flow,  $Q_c$ , as well as the chosen coefficients,  $\sigma$  and  $\phi$ , the pump dimensions, and the angular velocity. It is to the derivation of the function for the circulatory flow we now turn our attention. To accomplish this, the radial pressure rise through the rotor is first determined, using the steady flow energy equation and continuity. Returning



to the control volumes previously used, we then write the governing equations of the radial motion and solve for the radial pressure rise in the open passage. Combination of these two relations gives us the solution we desire.

Referring to Figure 10 a), page 34, for steady flow the resulting external torque on the fluid momentarily occupying a fixed differential control volume by Newton's second law is:

$$dT = dM(r_2 \sigma U_2 - r_1 \alpha C U_1) + R a \frac{\partial p}{\partial \theta} d\theta$$

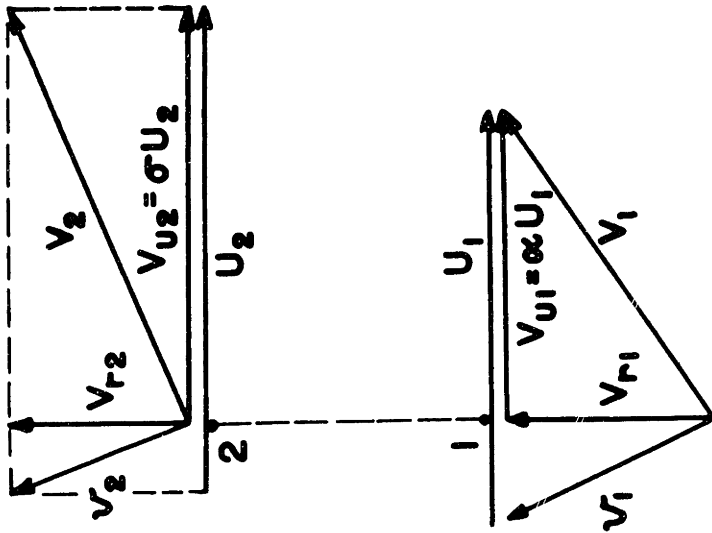
Since the forces acting on the rotor by Newton's third law must be equal, opposite, and collinear to those acting on the fluid enclosed by the rotor at any instant,

$$dW_s = dW_{in} = dT\omega$$

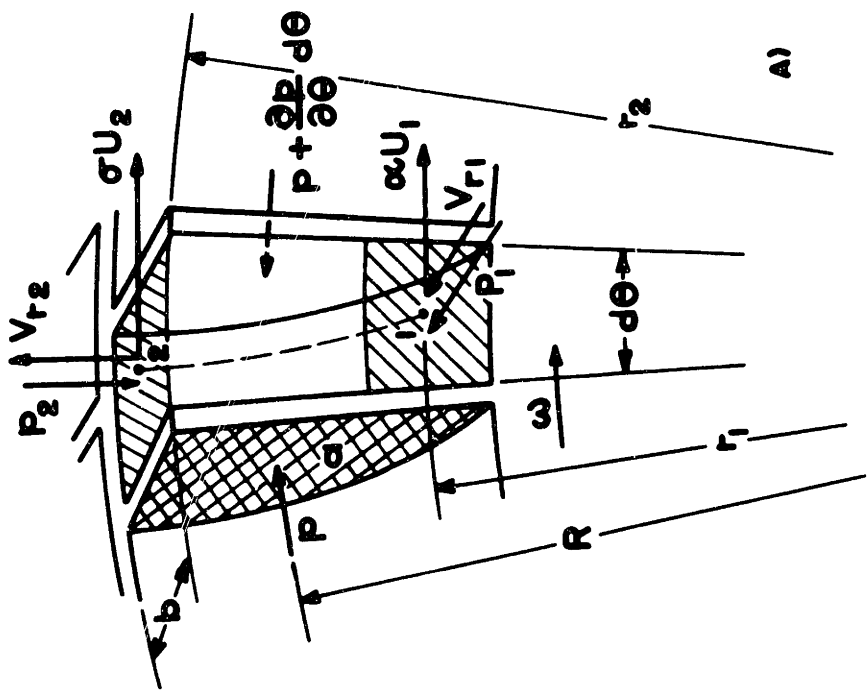
where  $dW_s$  is the shaft work, and  $dW_{in}$  is the work input to the fluid.

$$dW_{in} = dM (\sigma U_2^2 - \alpha C U_1^2) + R a \omega \frac{\partial p}{\partial \theta} d\theta \quad (16)$$

The first term on the right of equation (16) is the work as given by Euler's pump and turbine equation. The second term is known as the turbine work and tends to drive the rotor counter to its rotation through the working section of the pump. Through the stripper between the suction and discharge, however, the pressure gradient is reversed, and the turbine work is almost completely recovered.



B) VELOCITY DIAGRAMS



A)

FIGURE 10

Figure 10 b) on page 34 shows typical velocity diagrams at the blade entrance and exit for a high capacity. Since the rotor blades are radial it can be seen that at point 1 the relative velocity,  $v_1$ , will suffer an abrupt change in direction upon entering the blades, with a resultant energy loss. For this loss, which we will call the blade entrance loss rather than the long-misused term "shock loss," we assume that the kinetic energy associated with the tangential component ( $U_1 - cU_1$ ) of the relative velocity is converted into unavailable energy:

$$\text{Blade entrance loss} = \frac{dM (1 - c)^2 U_1^2}{2}$$

In the "ideal" model this is the only loss considered. With this term the steady flow energy relation for the control volume of Figure 10 a) becomes,

$$dW_{in} = dM \left[ \frac{V_2^2 - V_1^2}{2} + \frac{p_2 - p_1}{\rho} + \frac{(1 - c)^2 U_1^2}{2} \right] +$$

$$+ R a \omega \frac{dp}{d\theta} d\theta \quad (17)$$

From continuity we derive, (see equation (9)),

$$dM = \rho b r_1 d\theta V_{r1} = \rho b r_2 d\theta V_{r2} = \rho Q_c d\theta$$

so that,

$$V_{r1} = \frac{Q_c}{b r_1}, \text{ and } V_{r2} = \frac{Q_c}{b r_2}$$

From the velocity triangles of Figure 10 b),

$$V_1^2 = c^2 U_1^2 + V_{r1}^2$$

and,

$$V_s^2 = \sigma^2 U_s^2 + V_{r_s}^2$$

Equating equation (17) to equation (16), performing the above substitutions, and solving for the pressure rise between points 1 and 2:

$$P_2 - P_1 = \frac{\rho}{2} \left[ (2 - \sigma) \sigma U_s^2 - U_1^2 + \frac{Q_0^2}{b^2} \left( \frac{r_2^2 - r_1^2}{r_1^2 r_2^2} \right) \right] \quad (18)$$

#### VIII. RADIAL PRESSURE RISE IN OPEN CHANNEL OF "IDEAL" MODEL

The projection of a mean streamline on the meridional plane will again be followed in a clockwise direction. Continuity in the radial direction, considered for the control volume between points 2 and 3 of Figure 6, page 18, gives us:

$$\rho b r d\theta V_r = \rho b (r + dr) d\theta \left( V_r + \frac{\partial V_r}{\partial r} dr \right)$$

$$\frac{\partial V_r}{\partial r} + \frac{V_r}{r} = 0$$

Also from continuity and the definition of  $Q_c$ ,

$$dM = \rho b r d\theta V_r = \rho Q_c d\theta \quad (19)$$

The relation above then tells us,

$$\frac{\partial V_r}{\partial r} = - \frac{Q_c}{b r^2} \quad (20)$$

Considering the forces pertaining to the radial motion acting on this control volume, Newton's second law in terms of momentum gives the relation:

$$\begin{aligned}
& (p + \frac{\partial p}{\partial r} dr) b(r + dr) d\theta - p b r d\theta - p b dr \frac{d\theta}{2} - \\
& - (p + \frac{\partial p}{\partial \theta} d\theta) b dr \frac{d\theta}{2} = dM V_r - dM(V_r + \frac{\partial V_r}{\partial r} dr) + \\
& + \rho b dr (V_u + \frac{\partial V_u}{\partial r} \frac{dr}{2})^2 d\theta
\end{aligned}$$

which reduces to,

$$\frac{\partial p}{\partial r} = \rho \frac{V_u^2}{r} - \frac{1}{b r} \frac{dM}{d\theta} \frac{\partial V_r}{\partial r}$$

Using equations (19) and (20),

$$\frac{\partial p}{\partial r} = \frac{\rho Q_c^2}{b^3 r^3} + \rho \frac{V_u^2}{r} \quad (21)$$

Since we have already derived an equation for the tangential velocity,  $V_u$ , as a function of the radius, this relation may be treated as an ordinary integral equation to determine the pressure rise between points 2 and 3. That is,

$$\int_{p_2}^{p_3} dp = \frac{\rho Q_c^2}{b^3} \int_{r_2}^{r_3} \frac{dr}{r^3} + \rho \int_{r_2}^{r_3} \frac{V_{u(s-s)}^2}{r} dr$$

Solving in part,

$$p_3 - p_2 = \frac{\rho Q_c^2}{2 b^3} \left( \frac{r_2^2 - r_3^2}{r_2^3 r_3^3} \right) + \rho \int_{r_2}^{r_3} \frac{V_{u(s-s)}^2}{r} dr \quad (22)$$

For the last term on the right side of this equation, the tangential velocity,  $V_{u(s-s)}$ , from equation (3), page 20, is,

$$V_{u(s-s)} = \frac{r_3}{r} \sigma U_3 - \phi \frac{b}{2} \left[ \frac{r_3^2 - r^2}{r} \right]$$

and,

$$V_{u(s-s)} = \left[ \frac{\phi^2 b^2 r_s^4}{4} + \phi b r_s^2 \sigma U_s + r_s^2 \sigma U_s^2 \right] \frac{1}{r_s} - \left[ \frac{\phi^2 b^2 r_s^3}{2} + \phi b r_s \sigma U_s \right] + \frac{\phi^2 b^2}{4} r_s^2$$

Referring to equations (2), page 20, and (8), page 29, we find that,

$$\phi = \frac{(r_s \sigma U_s - r_1 c U_1)}{r_{cg} A}$$

Since,

$$U_1 = r_1 \omega, \text{ and } U_s = r_s \omega$$

let,

$$\phi = \frac{\sigma r_s^2 - c r_1^2}{r_{cg} A} \omega = \bar{\phi} \omega \quad (23)$$

Also, we define

$$C_1 = \bar{\phi} b r_s + 2 \sigma r_s$$

With these substitutions the previous equation simplifies to:

$$\frac{V_{u(s-s)}}{r} = \left[ \frac{C_1^2 r_s^2}{4 r_s} - \frac{\bar{\phi} b r_s C_1}{2 r} + \frac{\bar{\phi}^2 b^2 r}{4} \right] \omega^2$$

We next perform the integration of the remaining term of equation (22).

$$\begin{aligned} \rho \int_{r_s}^{r_s} \frac{V_{u(s-s)}}{r} dr &= \frac{\rho C_1^2 r_s^2 \omega^2}{4} \int_{r_s}^{r_s} \frac{dr}{r_s} - \\ &- \frac{\rho \bar{\phi} b r_s C_1 \omega^2}{2} \int_{r_s}^{r_s} \frac{dr}{r} + \frac{\rho \bar{\phi}^2 b^2 \omega^2}{4} \int_{r_s}^{r_s} r dr \\ &= \frac{\rho C_1^2 r_s^2 \omega^2}{8} \left( \frac{r_s^2 - r_s^2}{r_s^2 r_s^2} \right) - \frac{1}{2} \rho \bar{\phi} b r_s C_1 \omega^2 \ln \frac{r_s}{r_s} + \\ &+ \frac{1}{8} \rho \bar{\phi}^2 b A_1 \omega^2 (r_s + r_s) \end{aligned}$$

With equation (22) this solution gives the equation

for the radial pressure rise between  $r_2$  and  $r_1$ :

$$\begin{aligned}
 p_2 - p_1 &= \frac{\rho Q_c^2}{2 b^3} \left( \frac{r_2^2 - r_1^2}{r_2^2 r_1^2} \right) + \frac{\rho C_1^2 r_2^2 \omega^2}{8} \left( \frac{r_2^2 - r_1^2}{r_2^2 r_1^2} \right) - \\
 &\quad - \frac{1}{2} \rho \frac{1}{2} b r_2 C_1 \omega^2 \ln \frac{r_2}{r_1} + \\
 &\quad + \frac{1}{8} \rho \frac{1}{2} b A_1 \omega^2 (r_2 + r_1)
 \end{aligned} \tag{24}$$

The pressure variation in the direction of the circulatory flow between points 3 and 4 and also points 5 and 1 will be governed by the forces acting in the axial direction. Comparison of the control volumes of Figure 7, page 21, and Figure 9, page 25, shows that in both cases the differential equations are of the same form and have identical solutions. Considering the control volume of Figure 7, by continuity,

$$\rho c r_2 d\theta v_z = \rho c r_1 d\theta \left( v_z - \frac{\partial v_z}{\partial z} dz \right)$$

or,

$$\rho c r d\theta \frac{\partial v_z}{\partial z} dz = 0$$

so that,

$$\frac{\partial v_z}{\partial z} = 0 \tag{25}$$

By momentum in the axial direction,

$$p c r_2 d\theta - \left( p + \frac{\partial p}{\partial z} dz \right) c r_1 d\theta = dM \left( v_z - \frac{\partial v_z}{\partial z} dz \right) - dM v_z$$

$$\frac{\partial p}{\partial z} c r d\theta dz = 0$$

$$\frac{\partial p}{\partial z} = 0 \tag{26}$$

That is, neither the velocity nor the pressure varies as we move axially along the projection of a mean stream line between points 3 and 4 and points 5 and 1. From this we may conclude that:

$$p_3 = p_4 \quad (27)$$

and

$$p_1 = p_5 \quad (28)$$

For the control volume of Figure 8 on page 23 continuity along the projection of a mean stream line on the meridional plane between points 4 and 5 is satisfied if,

$$\rho \, d r \, d\theta \, V_r = \rho \, d (r + dr) \, d\theta \left( V_r + \frac{\partial V_r}{\partial r} dr \right)$$

which again gives us the relation,

$$\frac{\partial V_r}{\partial r} + \frac{V_r}{r} = 0$$

Since also from continuity and the definition of  $Q_c$ ,

$$dM = \rho \, d r \, d\theta \, V_r = \rho \, Q_c \, d\theta \quad (29)$$

we have by substitution,

$$\frac{\partial V_r}{\partial r} = - \frac{Q_c}{d r^2} \quad (30)$$

By Newton's second law of motion in terms of momentum, in the radial direction:

$$\left( p + \frac{\partial p}{\partial r} dr \right) d(r + dr) d\theta - p \, d r \, d\theta - p \, d dr \, d\theta =$$

$$dM \, V_r - dM \left( V_r + \frac{\partial V_r}{\partial r} dr \right) + \rho \, d dr \, d\theta \, V_u^2$$

Dropping those quantities small to thesecond order and



substituting from the continuity relations above,

$$\frac{\partial p}{\partial r} = \frac{\rho Q_c^2}{d^3 r^3} + \frac{\rho V_u^2}{r} \quad (31)$$

Since we again have an equation for the tangential velocity as a function of the radius,  $r$ , equation (31) may be integrated between proper limits to determine the pressure difference. Noting from Figure 4 b) on page 15 that  $r_4 = r_3$  and  $r_5 = r_1$ , and using equations (27) and (28),

$$\int_{p_2}^{p_3} dp = \frac{\rho Q_c^2}{d^3} \int_{r_1}^{r_3} \frac{dr}{r^3} + \rho \int_{r_1}^{r_3} \frac{V_{u(4-5)}^2}{r} dr \quad (32)$$

The square of the relation for  $V_{u(4-5)}$ , equation (5) on page 24, is quite long.

$$\begin{aligned} V_{u(4-5)}^2 = & \left\{ r_3^2 \sigma^2 U_3^2 - \phi r_3 \sigma U_3 \left[ A_1(r_3 + r_2) + 2 A_2 r_2 + \right. \right. \\ & \left. \left. + d r_2^2 \right] + \frac{\phi^2}{4} \left[ A_2^2 (r_3 + r_2)^2 + 4 A_2^2 r_2^2 + 4 A_1 A_2 r_2 (r_3 + r_2) + \right. \right. \\ & \left. \left. + 2 A_1 d r_2^2 (r_3 + r_2) + 4 A_2 d r_2^2 + d^2 r_2^4 \right] \right\} \frac{1}{r^3} - \\ & - \left\{ \frac{\phi^2}{4} \left[ 2 A_1 d (r_3 + r_2) + 4 A_2 d r_2 + 2 d^2 r_2^2 \right] - \phi r_3 \sigma U_3 d \right\} + \\ & + \frac{\phi^2 d^2}{4} r^2 \end{aligned}$$

To simplify, let,

$$\phi = \frac{1}{2} \omega, \text{ as defined by equation (23)}$$

$$C_3 = A_1(r_3 + r_2) + 2 A_2 r_2 + d r_2^2$$

$$\text{and } C_2 = \frac{1}{2} \frac{1}{2} C_3 - r_3^2 \sigma$$

With these substitutions,

$$\frac{V_{u(4-5)}^2}{r} = \left[ \frac{C_3^2}{r^3} - \frac{\frac{1}{2} d C_3}{r} + \frac{\frac{1}{4} d^2 r}{4} \right] \omega^2$$

and the solution of equation (32) gives us,

$$\begin{aligned}
 p_2 - p_1 = & \frac{\rho C_3^2 \omega^2}{2} \left( \frac{r_2^2 - r_1^2}{r_1^2 r_2^2} \right) - \rho \frac{\Phi}{2} d C_3 \omega^2 \ln \frac{r_2}{r_1} + \\
 & + \frac{1}{8} \rho \frac{\Phi^2}{2} d A_3 (r_2 + r_1) \omega^2 + \frac{\rho Q_c^2}{2 d^3} \left( \frac{r_1^2 - r_2^2}{r_1^2 r_2^2} \right)
 \end{aligned} \quad (33)$$

To determine the radial pressure rise in the open channel between points 1 and 2 we subtract equation (33) from equation (24):

$$\begin{aligned}
 p_2 - p_1 = & (p_2 - p_1) - (p_2 - p_1) \\
 p_2 - p_1 = & \frac{\rho C_3^2 \omega^2}{2} \left( \frac{r_2^2 - r_1^2}{r_1^2 r_2^2} \right) - \rho \frac{\Phi}{2} d C_3 \omega^2 \ln \frac{r_2}{r_1} + \\
 & + \frac{1}{8} \rho \frac{\Phi^2}{2} d A_3 (r_2 + r_1) \omega^2 + \frac{\rho Q_c^2}{2 d^3} \left( \frac{r_2^2 - r_1^2}{r_1^2 r_2^2} \right) - \\
 & - \frac{\rho Q_c^2}{2 b^3} \left( \frac{r_2^2 - r_1^2}{r_1^2 r_2^2} \right) - \frac{\rho C_1^2 r_2^2 \omega^2}{8} \left( \frac{r_2^2 - r_1^2}{r_1^2 r_2^2} \right) + \\
 & + \frac{1}{2} \rho \frac{\Phi}{2} b r_2 C_1 \omega^2 \ln \frac{r_2}{r_1} - \frac{1}{8} \rho \frac{\Phi^2}{2} b A_1 (r_2 + r_1) \omega^2
 \end{aligned} \quad (34)$$

#### IX. CIRCULATORY FLOW EQUATION OF "IDEAL" MODEL

Equation (34) above and equation (18) on page 36 are independent equations expressing the radial pressure difference between points 1 and 2 on the meridional projection of a mean stream line. Equating these relations, we obtain the desired equation for the circulatory flow,  $Q_c$ , as a function of  $\omega$ ,  $\Phi$ , pump dimensions, and the angular velocity of the rotor. Combining terms in a convenient form,

$$\begin{aligned}
 \frac{Q_c}{\omega} \left[ \frac{r_3^3 - r_1^3}{b^3 r_1^3 r_3^3} - \frac{r_3^3 - r_1^3}{d r_1^3 r_3^3} + \frac{r_3^3 - r_1^3}{b^3 r_3^3 r_1^3} \right] &= r_1^3 - (2 - \sigma) \sigma r_3^3 + \\
 + C_2 \left( \frac{r_3^3 - r_1^3}{r_1^3 r_3^3} \right) - 2 \frac{1}{2} d C_2 \ln \frac{r_3}{r_1} - \frac{C_1 r_3^3}{4} \left( \frac{r_3^3 - r_1^3}{r_3^3 r_1^3} \right) + \\
 + \frac{1}{4} A_3 d (r_3 + r_1) - \frac{1}{4} A_1 b (r_3 + r_1) + \frac{1}{2} b r_3 C_1 \ln \frac{r_3}{r_1}
 \end{aligned} \tag{35}$$

where, as previously defined:

$$\frac{1}{2} = \frac{\sigma r_3^3 - \sigma r_1^3}{r_{cg} A}$$

$$C_1 = \frac{1}{2} b r_3 + 2 \sigma r_3$$

$$C_2 = A_1 (r_3 + r_1) + 2 A_3 r_3 + d r_3^3$$

$$\text{and } C_3 = \frac{1}{2} \frac{1}{2} C_2 - r_3^3 \sigma$$

#### X. EFFICIENCY OF "IDEAL" MODEL

The increment of work input to the fluid in a differential angle  $d\theta$  was given by equation (16) on page 33. For the total working angle of both sides of the impeller, using the definition of  $Q_c$  and the derived relation for  $\Delta H_{tang}$ ,

$$W_{in} = 2 Q_c (\sigma U_3^3 - \sigma U_1^3) + 2 R a \omega \Delta H_{tang}$$

Since,

$$\Delta H_{tang} = \frac{Q_c (r_3 \sigma U_3 - r_1 \sigma U_1)}{r_{cg} A}$$

by substitution,

$$W_{in} = 2 r_{cg} A \omega \Delta H_{tang} + 2 R a \omega \Delta H_{tang}$$

We define:

$$Q_s = 2 r_{cg} A\omega \quad (36)$$

and,

$$Q_r = 2 R a\omega \quad (37)$$

The first term,  $Q_s$ , is seen to be the flow the pump would deliver if solid body rotation with respect to rotor velocities was obtained. The second term,  $Q_r$ , represents the fluid within the vanes carried through the stripper. With these definitions,

$$W_{in} = Q_s \Delta H_{tang} + Q_r \Delta H_{tang} \quad (38)$$

Before the efficiency equation can be written the concept of useful work must be considered. An accepted definition of the useful work of a pump or compressor is the product of the capacity and the total head. Under this definition the turbine work, which is the second term on the right of equation (38), must necessarily be treated as an internal phenomenon. As stated before, the turbine work acting against rotation through the working section is balanced in large part by the torque it produces at the stripper between discharge and suction. To be consistent in the definition of hydraulic efficiency of the overall pump, only the loss in this internal transfer of energy should be considered. In the "ideal" model, of course, no such loss occurs. By this reasoning the work input is simply,

$$W_{in} = Q_s \Delta H_{tang} \quad (39)$$

and the hydraulic efficiency,

$$\eta_h = \frac{Q \Delta H_{tang}}{Q_s \Delta H_{tang}}$$

$$\eta_h = \frac{Q}{Q_s} \quad (40)$$

### XI. ANALYSIS OF AN "IDEAL" MODEL

In the analysis we have determined relations for the major quantities which describe the operation of our "ideal" model: capacity,  $Q$ ; total head,  $\Delta H_{tang}$ ; work input,  $W_{in}$ ; circulatory flow,  $Q_c$ ; and efficiency,  $\eta_h$ . Each of these terms can be shown to reduce to functions of the chosen coefficients,  $\alpha$  and  $\sigma$ , which relate the tangential velocity of the fluid to that of the rotor at points 1 and 2 respectively; of the rotor speed,  $\omega$ ; and of the pump dimensions. Two of these equations as derived are much too long and involved to be repeated at this point for easy reference. Without loss of meaning we may, however, reduce these equations using the dimensions of the unit investigated in the experiments, the Sta-Rite 1 $\frac{1}{2}$  TH-7, and a chosen speed of 3600 rpm. The dimensions of the test model are given in the Appendix. Our fundamental relations are:

$$(10) \quad \Delta H_{tang} = \frac{Q_c (r_1 \sigma U_1 - r_2 \alpha U_2)}{r_{cg} A} = (1129.77 \sigma - 591.77 \alpha) Q_c$$

.....  $\frac{\text{ft.-}\#}{\text{lb.}}$

$$(15) \quad Q = .2187 \sigma + .1394 \alpha \dots \dots \dots \text{ft}^3/\text{sec}$$

$$(35) \quad 364 Q_c^2 = 124.3 \sigma^2 + 21.77 \alpha \sigma - 223.2 \sigma + 12.94 \alpha^2 - 58.45$$

.....  $\frac{\text{ft.-}\#}{\text{lb.}}$

$$(39) \quad W_{in} = Q_s \Delta H_{tang} = .3947 \Delta H_{tang} \dots \dots \dots \text{ft.-}\#/\text{sec}$$

$$(40) \quad \eta_h = \frac{Q}{Q_s} = \frac{Q}{.3947}$$

(We retain original equation designations for easy back reference.)

From the similitude relations it is known that the mechanics of operation are independent of the viscous forces. That is, the ratio of any characteristic pressure force to dynamic force is dependent only on a characteristic kinematic parameter. In our derivations, since  $\sigma$  is assumed to be constant, the characteristic parameter is  $\alpha$ . Referring to equation (15), it is seen that capacity increases with  $\alpha$ . From observation, using a directional probe, it was found that  $\alpha$  is positive at high flows. Again from equation (15) at shut off (maximum head) where the capacity,  $Q$ , is zero,  $\alpha$  must necessarily be negative. This reversal in direction of the tangential velocity at the blade entrance as capacity varies is in agreement with observation. A comparison of the theoretical and experimental flow angles for the actual pump is shown in the results.

In equation (10) for the total head, this variation in tangential velocity as represented by  $\omega$  is seen as the apparent cause of the sharply rising head curve as capacity decreases. However, as discussed in the hypothesis of operation, the rate of the circulatory flow may be expected to increase continuously as we approach shut off, thereby further steepening the head curve.

Unlike the centrifugal pump, the regenerative pump demands more rather than less power as shut off conditions are approached. Along with the total head, this characteristic also parallels the performance of a rotary positive displacement pump. Equation (39) qualitatively satisfies the observed performance since the work input is proportional to the total head.

It is known that the maximum capacity as a pump corresponds to zero pressure rise. In our discussion it has been reasoned that pressure rise is directly proportional to circulatory flow. Returning to equation (10), we see that the total head will equal zero when the circulatory flow is zero, or when

$$r_2 \sigma U_2 = r_1 \omega U_1$$

that is, using the definitions of  $\omega$  and  $\sigma$ , when

$$V_{u1} = \frac{r_2}{r_1} V_{u2}$$

This relationship states that the forward tangential velocity of the fluid at the blade entrance is greater

than the velocity leaving the blade tip. This would result in an external centrifugal field stronger than that produced by the rotor, resulting in a reversed circulatory flow. The only occasion when  $V_{u1}$  may be greater than  $V_{u2}$  is when it is reversed from the direction of the rotation (low capacity) under the influence of the pressure gradient. The point of zero head must then occur in the "ideal" model when the circulatory flow is zero.

For the case of no circulatory flow, the centrifugal head developed by the radial legs of the flow path within and without the rotor must be equal and opposite. Setting  $Q_c$  equal to zero in equation (35) satisfies this condition. The value of  $\sigma$  for the "ideal" model of the test pump may be reasonably assumed as unity in this equation, that is, we propose in the "ideal" case a rotor having an infinite number of blades of infinitesimal thickness. Solving equation (35) with these conditions gives us at maximum capacity,

$$12.94 \alpha^3 + 21.77 \alpha - 40.45 = 0$$

$$\alpha = 1.115; - 2.801$$

where only the positive value is the root of interest, since from equation (15) at shut off ( $Q = 0$ )  $\alpha$  equals -1.569, the lowest value in the operating range of the pump.

Substitution of equation (15) in equation (40) discloses that the efficiency is a straight line function



increasing with  $cC$ , therefore reaching maximum efficiency as a pump at maximum capacity. The flow  $Q$  found from equation (15) for the upper value of  $cC$  (1.115), considering the effect of the blade entrance loss, corresponds to the expected hypothetical flow rate for zero pressure, that is, for an "ideal" efficiency of nearly 100 percent.

Solutions for the capacity and efficiency over the operating range of the "ideal" model can be seen to be possible. Substitution of permissible values within the range of the variable  $cC$  in equation (35), however, results in imaginary answers for the circulatory flow over most of the hypothetical operating range of the pump. Therefore a complete solution for values of the circulatory flow, and hence the total head, is not possible.

A preliminary analysis, assuming completely reversible processes within the pump (including no blade entrance loss) produced no real solutions at all for the circulatory flow in the working range. This was clearly related to the incompatibility of the efficiency relation, equation (40), which indicates efficiencies less than unity for a model without irreversibilities. Since the efficiency is directly dependent on the assumption of identical mechanics throughout the working section of the pump, this assumption must be incompatible with zero

irreversibilities. That is, a constant value for the circulatory flow per unit angle cannot exist. Rather than abandon this assumption, however, which is consistent with the observed linear tangential pressure gradient, we choose to modify our conception of an "ideal" model by introducing further irreversibilities.

## XII. INTRODUCTION OF FRICTION IN EQUATIONS OF MOTION

Irreversibilities are first introduced in the analysis by the addition of shear forces to the typical differential control volume. The hypothesis of operation and the remaining assumptions pertaining to the "ideal" model are retained. As shown in the Appendix, page 77, the new differential equations of motion written in their simplest form are non-linear first-order functions. In this example, the equation for the tangential velocity between points 2 and 3 is derived and is determined as the ratio of Bessel functions, or series solutions. Later derivations require the squaring and integration of this already complicated result. This involvement is inconsistent with our original simplifying assumptions, and physical interpretation of the resulting equations cannot readily be made.

### XIII. ANALYSIS OF A "REAL" MODEL

Although it was not possible to obtain a solution of the "ideal" model compatible with the known mechanics, the analysis informed us that the equations for capacity, head, and work input were basically sound in the light of observed performance. A modification of our idealization to a "real" regenerative pump with irreversibilities was deduced to be necessary. However, it was determined that the addition of shear forces in the original differential equations of motion was analytically impractical.

Theoretical performance curves which are in remarkable agreement with those obtained by experiment are reached quite readily if we assume shear effects will not alter the mean tangential velocity profile.

Let us consider a unit where we have shear losses in the inlet and discharge and through the rotor at all times. However, in the first step it is assumed there is no fluid shear affecting the motion in the open channel. The pump is then operating at some value of head and capacity, and  $cC$  and  $\sigma$  have particular values. Next, assume shear forces are added in the open channel. The unit is now operating at a new value of head and capacity, and  $cC$  has changed. Since this is an actual pump, some "slip" occurs and  $\sigma$  has a value less than unity. However,  $\sigma$  is assumed a function of only the design of the rotor and its value is constant in all cases. We next open

or close the pump discharge valve, as required, to adjust the flow conditions until  $cC$  is again the same value as before friction is added in the open channel. Again the head and capacity will alter. If fluid shear has not changed the tangential velocity distribution to a great extent, the capacity will have approximately the same value as without friction.

To investigate this possibility we first consider identical meridional sections of the open channel for the case without friction and for the case with friction after the flow has been adjusted to the original  $cC$ . The losses associated with the thru-flow will be largely caused by the inlet, discharge, and channel surfaces, while the losses associated with the circulatory flow, other than the blade entrance loss, will be mainly caused by irreversibilities through the rotor. We therefore assume that the radial and tangential losses are independent, and that the radial shear losses in the open channel are very small in comparison with the blade entrance loss and the radial shear loss through the rotor. That is, if the tangential velocities outside the rotor are relatively unchanged, so that the external centrifugal field is the same, the quantitative value of the circulatory flow will be essentially unaltered by a small addition of friction. With this stipulation, since  $cC$  and  $\sigma$  are identical with and without friction, the total

angular momentum change through both meridional sections will be the same. In terms of the tangential pressure gradients, we find,

$$\left[ \left( \frac{dp}{d\theta} \right)_{\text{friction}} \right]_{\text{without}} = \left[ \left( \frac{dp}{d\theta} \right)_{\text{useful}} + \left( \frac{dp}{d\theta} \right)_{\text{friction}} \right]_{\text{with}} \quad (41)$$

Consider next any typical differential control volume within each of the identical meridional sections. From experiment for an actual pump and by assumption for an "ideal" model we have stated that the tangential pressure gradient,  $\frac{dp}{d\theta}$ , is not only independent of angular position,  $\theta$ , but also independent of radius,  $r$ . From the latter condition we conclude that the tangential pressure gradient across a differential control volume is the same as that across a meridional section, and so equation (41) pertains to compared differential control volumes as well. The change in angular momentum through a differential control volume with and without friction must then be the same, and we may finally deduce that the tangential velocity profile is not altered by shear effects.

The accuracy of the above conclusion is dependent on the assumptions, which we will apply in the analysis, concerning the losses in the unit. Under these conditions, the tangential velocity equations of the "ideal" model are retained. The previous equation for the capacity must then apply equally well to the "real" pump. Repeating from page 46 for the Sta-Rite 1 $\frac{1}{2}$ -TH-7 at 3600 rpm,

$$(15) \quad Q = .2187 \sigma + .1394 \alpha C \dots \dots \dots, \text{ft}^3/\text{sec}$$

(Original equation designations will again be used wherever applicable for easy back reference.)

As another consequence of keeping the ideal velocity profile, the centrifugal field set up in the open channel is unaltered. Equation (34) on page 42 for the radial pressure rise in the open channel then differs from that actually obtained only in a shear loss term in the radial direction. Adding a radial loss term and using the dimensions of the test pump in equation (34), we obtain:

$$\Delta H_{1-2} = 12.75 \sigma^2 + 21.77 \alpha C \sigma + 12.94 \alpha C^2 + 400.87 Q_c^2 - \Delta H_{fr.rad.} \dots \frac{\text{ft.} - \#}{\text{lb.}} \quad (42)$$

Blade entrance losses through the rotor have already been taken into account. Introducing a head loss term in the relation derived using the steady flow energy equation changes equation (18) on page 36 only to the extent of the addition of the radial shear loss. Introducing pump dimensions:

$$\Delta H_{1-2} = 111.58(2 - \sigma) \sigma - 58.45 + 764.84 Q_c^2 - \Delta H_{fr.rad.} \dots \frac{\text{ft.} - \#}{\text{lb.}} \quad (43)$$

Combining equations (42) and (43) and adding the two radial shear losses,

$$\Delta H_{fr.rad.} - 364 Q_c^2 = 223.2 \sigma - 124.3 \sigma^2 - 21.77 \alpha C \sigma - 12.94 \alpha C^2 - 58.45 \dots \frac{\text{ft.} - \#}{\text{lb.}} \quad (44)$$

Within our hypothesis this equation will determine  $Q_c$  once  $\Delta H_{fr.rad.}$  and the "coefficient of slip,"  $\sigma$ , are evaluated.

Turning our attention to the relation for the total head of the "ideal" model on page 45,

$$(10) \quad \Delta H_{tang.} = (1129.77 \sigma - 591.77 \alpha) Q_c \dots \frac{ft.-\#}{lb.}$$

we conclude that use of the value of  $Q_c$  from equation (44) in this expression now gives us the total head developed by the pump after radial losses are considered but before tangential losses are accounted for. That is,

$$\Delta H_{tang.} = TH + \Delta H_{fr.tang.} \quad (45)$$

where TH is the total head actually developed by the "real" pump,\* and the loss term includes inlet and discharge losses, irreversibilities through the stripper associated with the turbine work, and head drop through the working section.

The work input at the rotor of the "real" pump is again only the Euler work as determined on page 44,

$$(39) \quad W_{in} = Q_s \Delta H_{tang.}$$

Substituting equation (44),

$$W_{in} = Q_s (TH + \Delta H_{fr.tang.}) \quad (46)$$

---

\* The change in "velocity head" across the test model is zero and the change in "gravity head" is negligible.

With the previous definition for useful work output the efficiency relation of page 45 is altered to,

$$\eta_h = \frac{Q}{Q_s} \left[ \frac{TH}{TH + H_{fr.tang.}} \right] \quad (47)$$

The new relations, (44) through (47), along with equation (15), now describe, within our two-dimensional analysis, the theoretical operation of the regenerative pump used in experiments by Lazo and Hopkins and by Lutz-- once the form of the radial and tangential loss terms is determined. Since the nature of the radial losses is unknown at this point very little can be deduced as to the variation of the circulatory flow from equation (44). Qualitatively, however, it may be reasoned that the circulatory flow of the "real" pump is quite large over the entire range of operation, including the maximum capacity point where the total head delivered is zero. At this point, the tangential shear loss through the inlet, working section, and discharge, would be maximum while at the same time the difference in tangential velocity between blade tip and root would be minimum. For the necessary change in angular momentum to overcome the shear loss, the circulatory flow must be still quite active at maximum capacity. We conclude that the flow pattern is always of a very turbulent nature, although well ordered in the mean. Further, similitude has demonstrated that the mechanics are independent of Reynolds number. We therefore assume



that the radial and tangential losses are proportional to the square of the flows in the respective directions:

$$\Delta H_{fr.tang.} = K_t Q^2 \quad (48)$$

$$\Delta H_{fr.rad.} - 364 Q_c^2 = K_r Q_c^2 \quad (49)$$

where  $K_t$  and  $K_r$  are the proportionality constants. In equation (49) we refer to the "net loss," that is, the actual radial head loss after momentum changes. An analogy would be the pressure loss through a pipe of varying cross-section, or a sudden expansion.

#### XIV. CORRELATION OF THEORY AND EXPERIMENTAL DATA

The theoretical analysis of the "real" pump cannot predict performance until the methods of pre-evaluating the constants  $K_t$ ,  $K_r$ , and  $\sigma$  are studied. This theoretical study will be considered in detail in the next phase of the regenerative pump project.

The validity of the theory can be satisfactorily substantiated, however, using experimental data to determine the three constants simultaneously, and comparing the resulting theoretical equations in all respects with experimental performance. These data are taken from results of air tests at 3600 rpm by Lazo and Hopkins. Since only three independent items of data are required, results from three points of the head-capacity curve are selected as the most important characteristic. Chosen are the

maximum capacity point where the actual total head is zero ( $Q = .305 \text{ ft}^3/\text{sec}$ ), the shut off point where capacity is zero ( $TH = 1210 \text{ ft.} \cdot \#/\text{lb.}$ ), and a third point at approximately fifty per cent capacity ( $Q = .150 \text{ ft}^3/\text{sec}$ ;  $TH = 740 \text{ ft.} \cdot \#/\text{lb.}$ ). The expressions obtained for the three constants are:

$$\frac{(2058.14 \sigma - 636.74) \sqrt{-122 \sigma^2 + 243.47 \sigma - 73.43}}{1.7007 \sigma \sqrt{-122 \sigma^2}}$$

$$\frac{-(497.93 \sigma - 313.23) \sqrt{-122 \sigma^2 + 264.4 \sigma - 120.39}}{+ 223.2 \sigma - 58.45} = 740$$

from which,

$$\sigma = .844$$

$$K_r = (1.7007)^2 \sigma^2 \sqrt{-122 \sigma^2 + 223.2 \sigma - 58.45} = 88.66$$

$$K_t = \frac{2058.14 \sigma - 1294.73}{.093} \sqrt{\frac{-122 \sigma^2 + 274.4 \sigma - 120.39}{K_r}} = 2011.46$$

The values of these constants when used in the original relations supply the following theoretical equations for the performance of the Sta-Rite  $1\frac{1}{2}$ -TH-7 at 3600 rpm:

$$(15) \quad Q = .1846 + .1394 \alpha$$

$$(44) \quad Q_c^2 = .4668 - .2072 \alpha - .1460 \alpha^2$$

$$(45) \quad TH = (953.53 - 591.77 \alpha) Q_c - 2011.46 Q_c^2$$

$$(46) \quad HP = \frac{(.0745)(.3947)}{550} (953.53 - 591.77 \alpha) Q_c$$

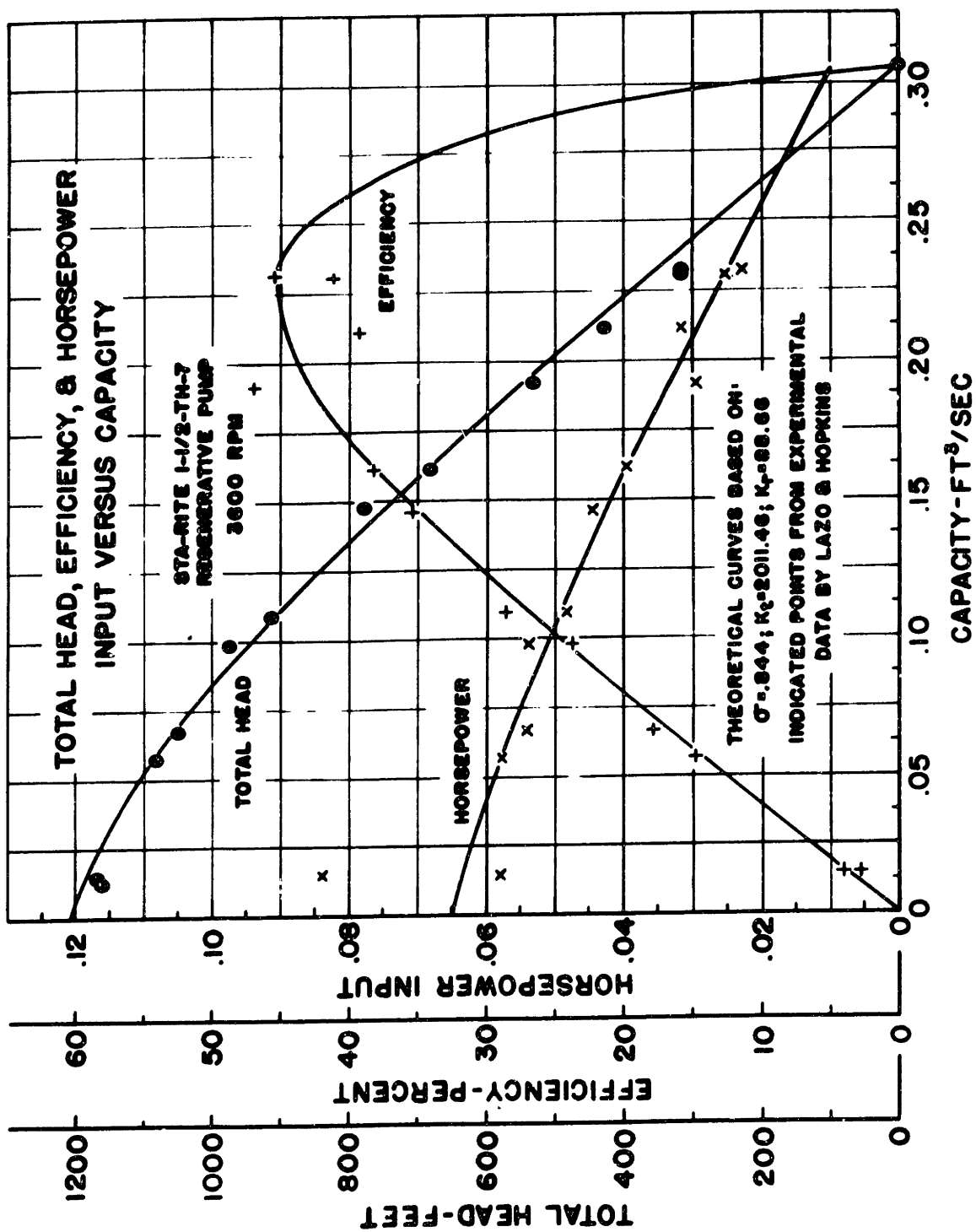
$$(47) \quad \eta_h = \frac{Q}{.3947} \frac{TH}{TH + 2011.46 Q_c^2}$$

where  $\alpha$  varies between .8637 at maximum capacity (.305  $\text{ft}^3/\text{sec}$ ) and -1.3242 at shut off. (To follow accepted

convention the capacity,  $Q$ , was used as the independent variable in Graphs 1, 5 and 6. and the dimensionless flow rate,  $Q/\omega D^3$ , in the remaining graphs.)

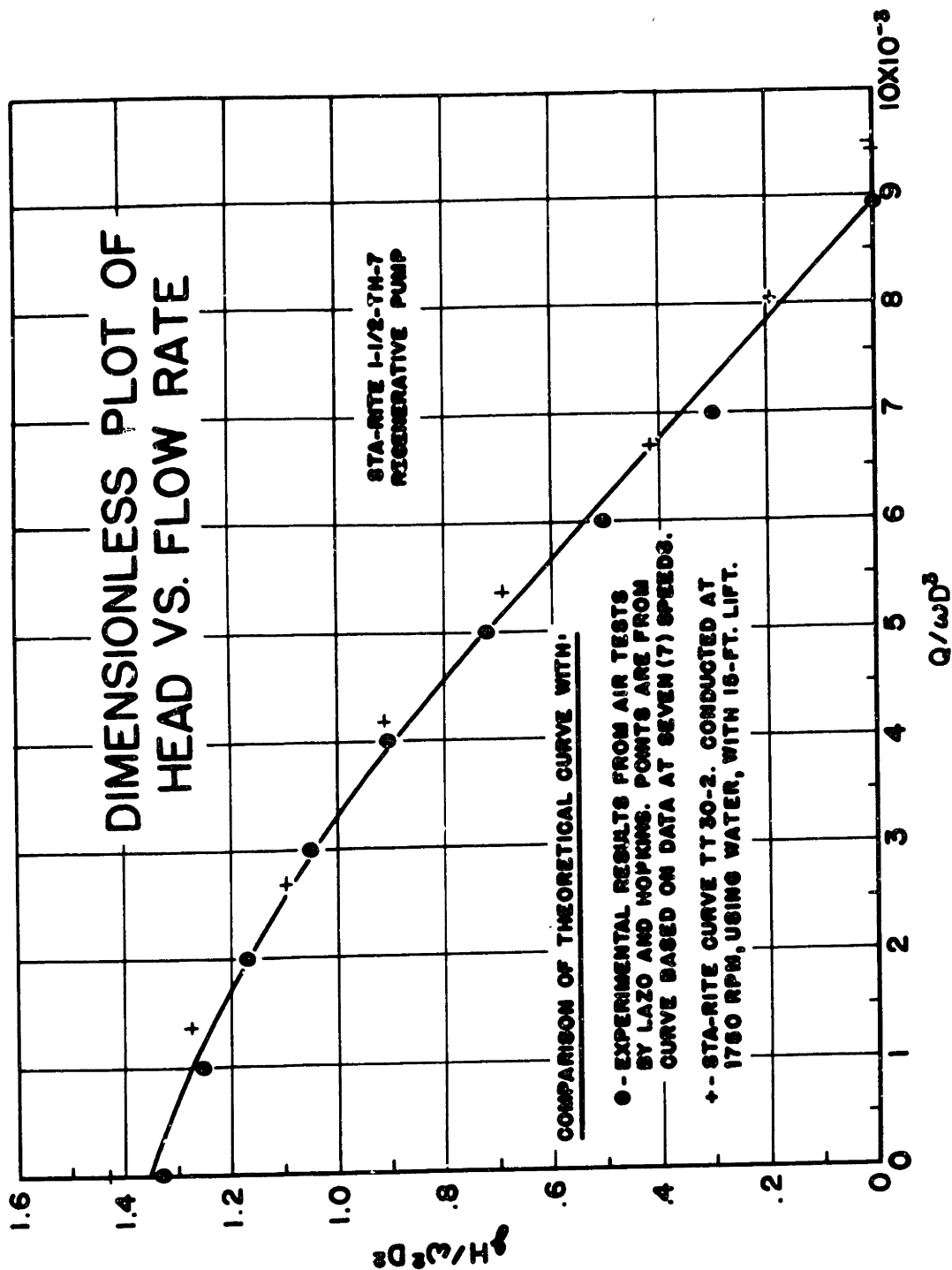
Correlation of theory and experiment is very remarkable, as demonstrated by Graphs 1 to 4. It is a significant fact that data were taken at widely separated points from only one of the primary performance curves to determine three independent constants. And yet, the theoretical equations agree with experimental data for the two independent characteristics, total head and horsepower input, as clearly shown in Graph 1, page 60, for the air tests conducted here at the Institute. This graph also indicates the experimental scatter which might be expected in a limited number of points at a particular speed. The final data used in evaluating the constants were adjusted to effect the same compromise among the scatter of the three curves as would be achieved using French curves.

It has been stated previously that the regenerative pump is a hydrodynamic unit. We can take advantage of this fact for a better comparison of the theoretical solution. Plotting the performance on a dimensionless basis allows the use of all data regardless of fluid pumped or speed. From the work by Lazo and Hopkins results are available from air tests at seven speeds ranging from 1200 rpm to 4800 rpm. The indicated points from the air tests on Graphs 2, 3, and 4, which immediately follow,



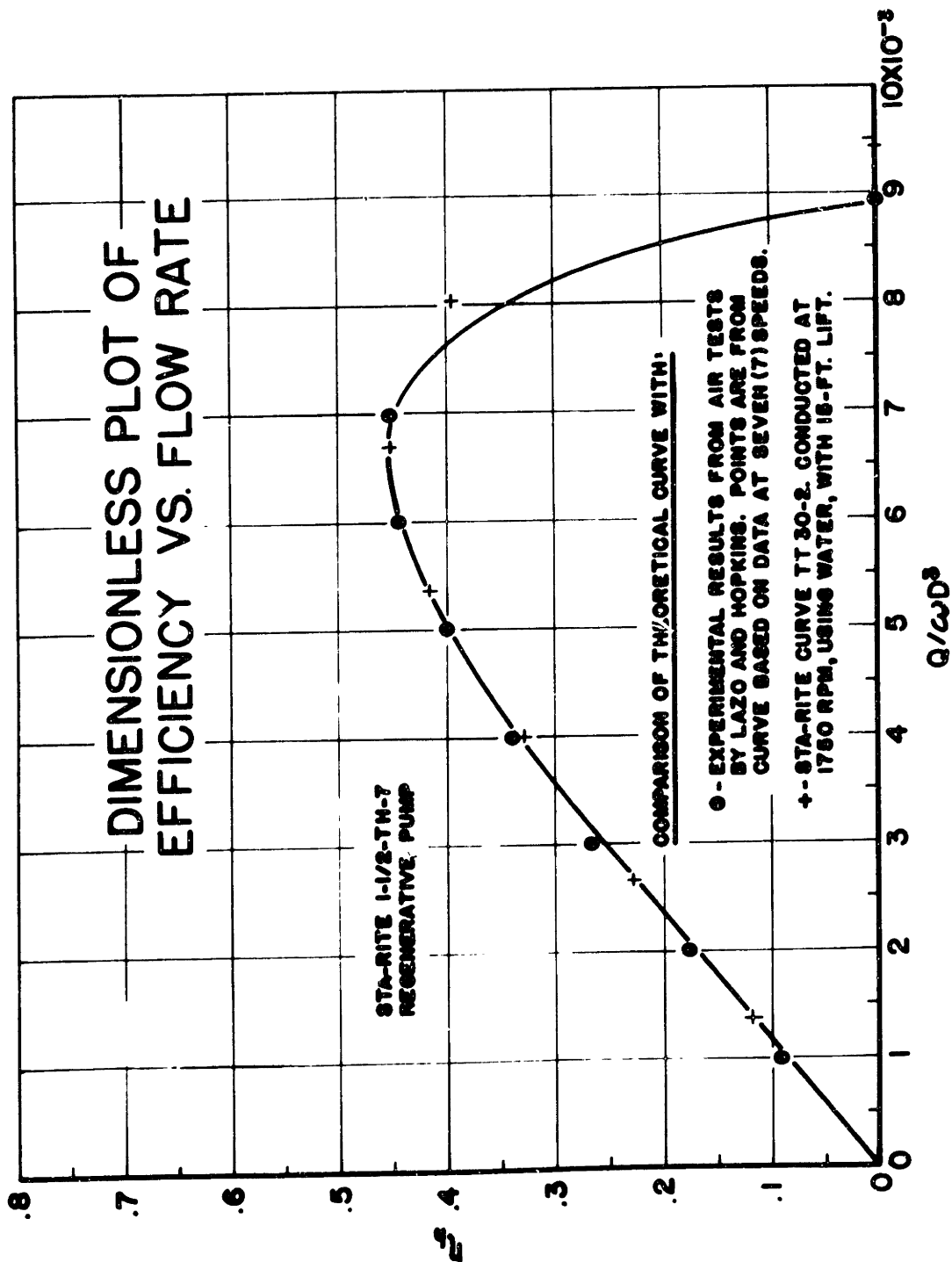
GRAPH 1

THEORETICAL AND EXPERIMENTAL PERFORMANCE AT 3600 RPM  
OF REGENERATIVE PUMP.

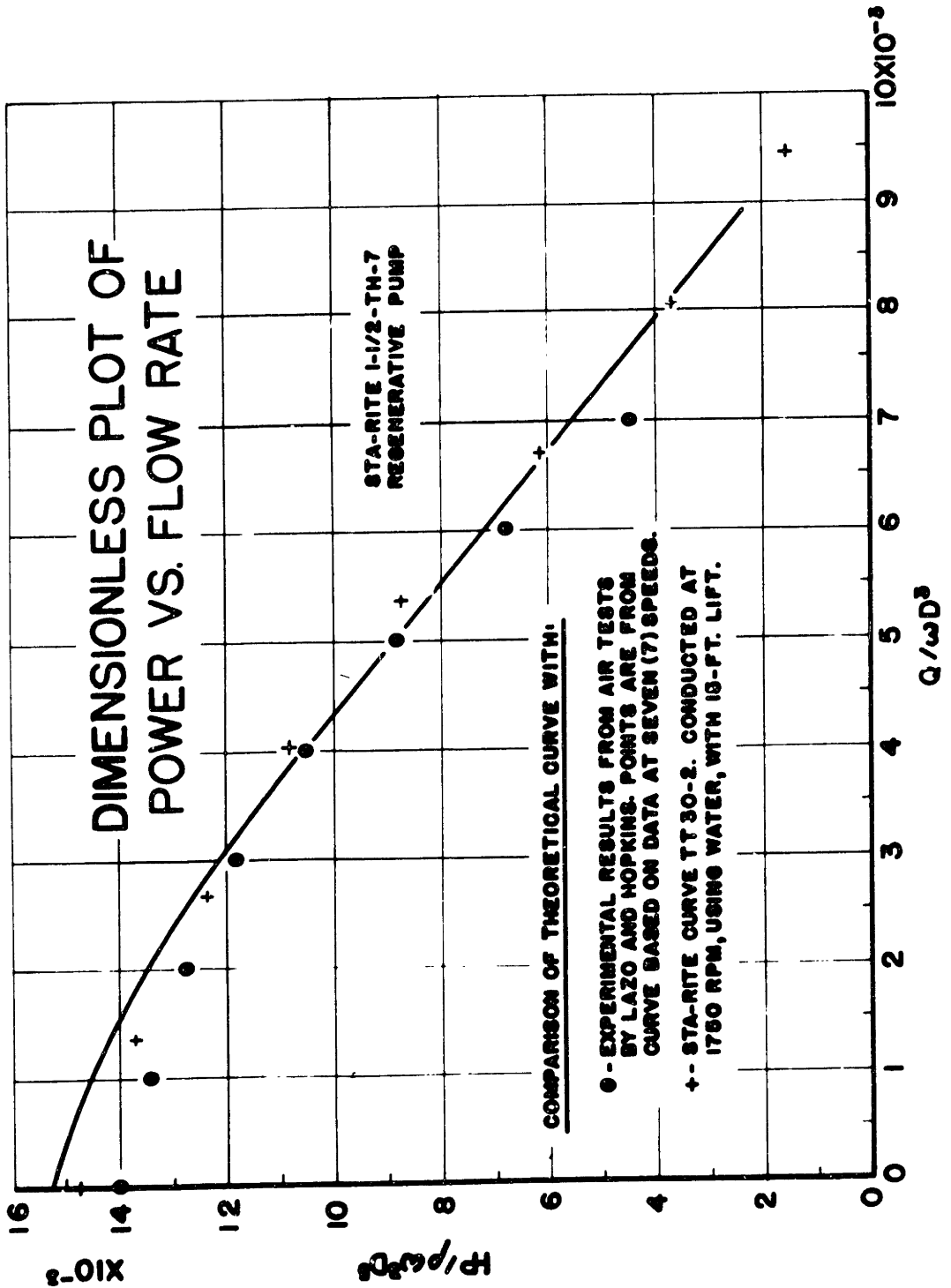


GRAPH 2

REGENERATIVE PUMP THEORETICAL DIMENSIONLESS HEAD COEFFICIENT COMPARED WITH AIR AND WATER EXPERIMENTS.

**GRAPH 3**

REGENERATIVE PUMP THEORETICAL EFFICIENCY  
COMPARED WITH AIR AND WATER EXPERIMENTS.



GRAPH 4

REGENERATIVE PUMP THEORETICAL DIMENSIONLESS POWER  
COEFFICIENT COMPARED WITH AIR AND WATER EXPERIMENTS.

are taken from the curve based on this wealth of information, thus reducing the experimental error. Points from an experimental curve made by the manufacturer, using an identical unit, are also shown. Sta-Rite's test was conducted at 1750 rpm, using water, with a constant 15-foot suction lift. The theoretical curves of these graphs are those of Graph 1 converted to a dimensionless basis. Correlation of the theoretical solution and the air and water tests can be seen to be excellent. One of the important facts substantiated by the results is that the constants may be considered independent of capacity as assumed, and unaffected by speed or fluid medium. The performance curves would, of course, break sharply if cavitation occurred, so speed and the type of fluid pumped are still important factors.

On page 19 the work of Busemann and of Stodola was referred to in connection with the "coefficient of slip"  $\sigma$ . The value of  $\sigma$  obtained from the theoretical solution agrees surprisingly well quantitatively with the work of these investigators as reported by Dr. Wislicenus.<sup>1</sup> From this source the Busemann factor for a radial-flow impeller with forty 90-degree blades is approximately 0.87 and the Stodola correction approximately 0.80. For both factors the effect of fluid shear was disregarded in the analysis

---

<sup>1</sup> Fluid Mechanics of Turbomachinery, McGraw-Hill, New York, 1947.



of the investigators, and the values are high for a real impeller. The value of  $\sigma$  determined by our theoretical solution was 0.844.

A number of assumptions are required to apply the work of these investigators to the regenerative pump. Comparison is based on the conditions that -

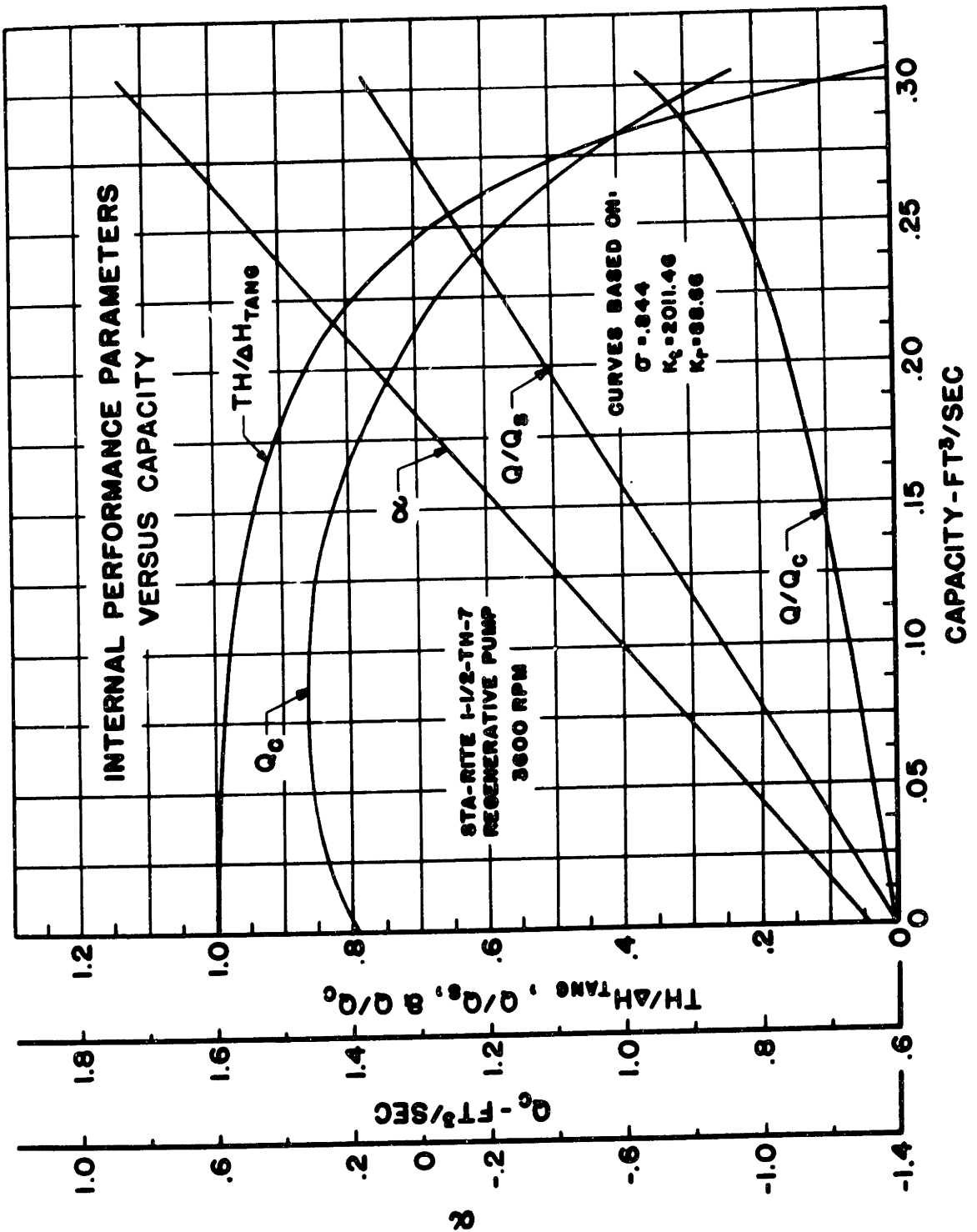
(1) The rotor may be considered shrouded. In the theoretical analysis the flow is assumed as though a barrier or shroud does exist.

(2) The ratio of blade length to spacing is great enough so that the coefficient of slip is determined entirely by the discharge portion of the vanes. For the test unit the ratio is 1.75:1.

(3) The coefficient of slip is independent of capacity.

The apparent agreement with these investigations for the regenerative unit studied may be coincidence. This is particularly so since the effects of dimensions and shape of liquid passage were not considered by Busemann and Stodola, and of course the actual regenerative rotor is unshrouded.

In Graph 5, page 66, a number of internal performance parameters from the theoretical solution are plotted at 3600 rpm for the test unit. The values for  $Q_c$  are for a double-sided or commercial pump, rather than for a single-flow unit used in the derivations. The trend of this curve

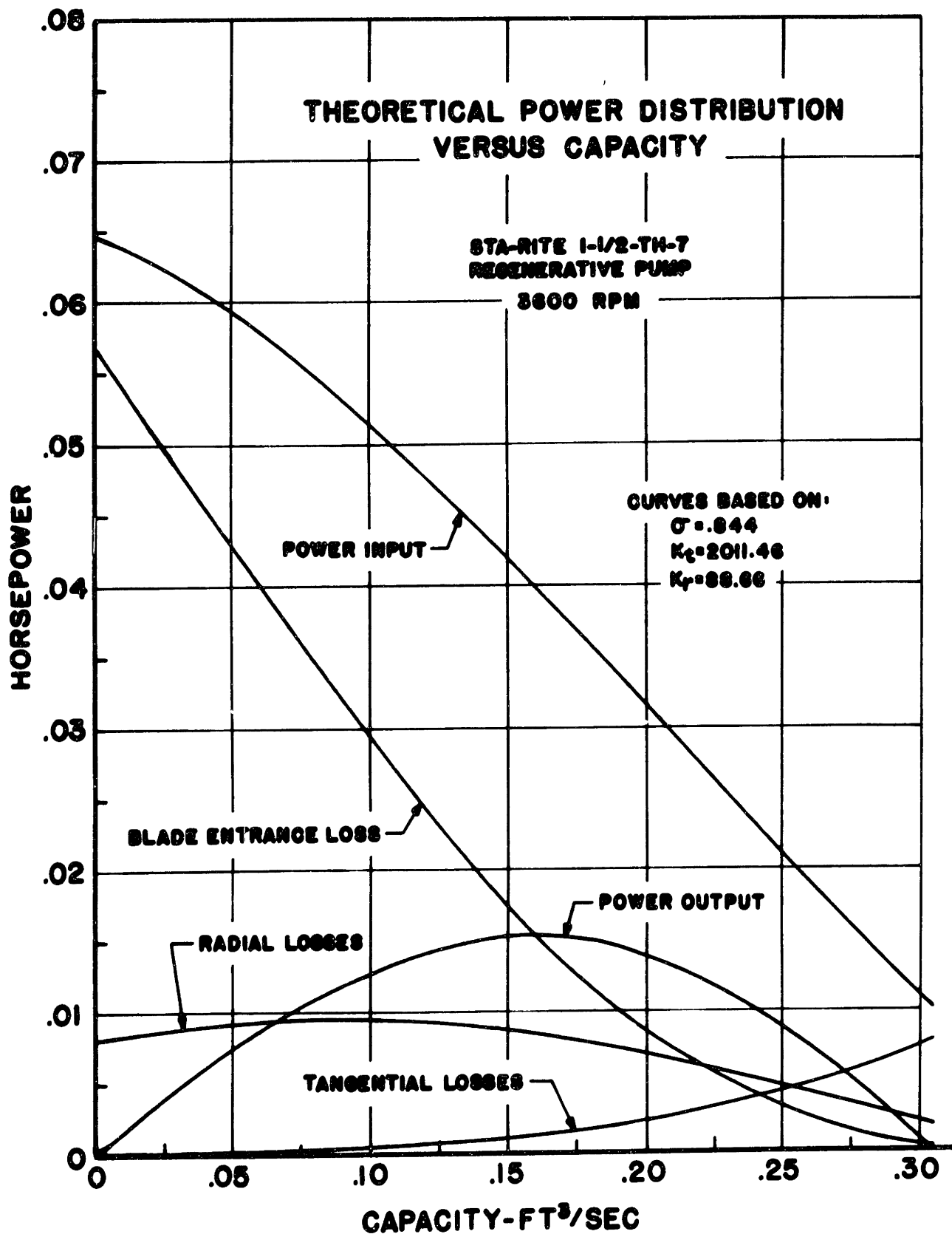


**GRAPH 5**  
 INTERNAL PERFORMANCE PARAMETERS AT 3600 RPM  
 OF REGENERATIVE PUMP.

shows that for the test unit  $Q_c$  does not continually increase as shut-off conditions are approached, but reaches a maximum at a capacity of about .09 ft<sup>3</sup>/sec. As indicated by the curve for  $\omega C$ , the tangential velocity of the fluid outside the rotor near the blade root decreases and then reverses under the influence of the pressure gradient. Near shut-off the centrifugal field produced by reversed tangential flow again approaches that produced by the rotor, reducing the circulatory flow.

From the study of the "ideal" model, the ideal efficiency was determined as the ratio of the capacity to the maximum capacity at solid body rotation,  $Q/Q_g$ . This curve on Graph 5, then, is an indication of the maximum efficiency that could be attained by the test model with its present design. The hydraulic efficiency of the "real" pump is the product of the values of the  $Q/Q_g$  curve and the  $TH/\Delta H_{\text{tang.}}$  curve. This latter curve depicts the ratio of the useful total head to the head developed after blade entrance and radial losses are considered, and reflects the effect of tangential losses in the pump.

A better picture of the losses is given by the power distribution curves of Graph 6, page 68. These curves are a result of the theoretical solution and may prove the most immediately useful in the improvement of the regenerative pump. The values of the horsepower are given for air with a specific mass of 0.0745 lbs/ft<sup>3</sup> from the experiments of Lazo and Hopkins.

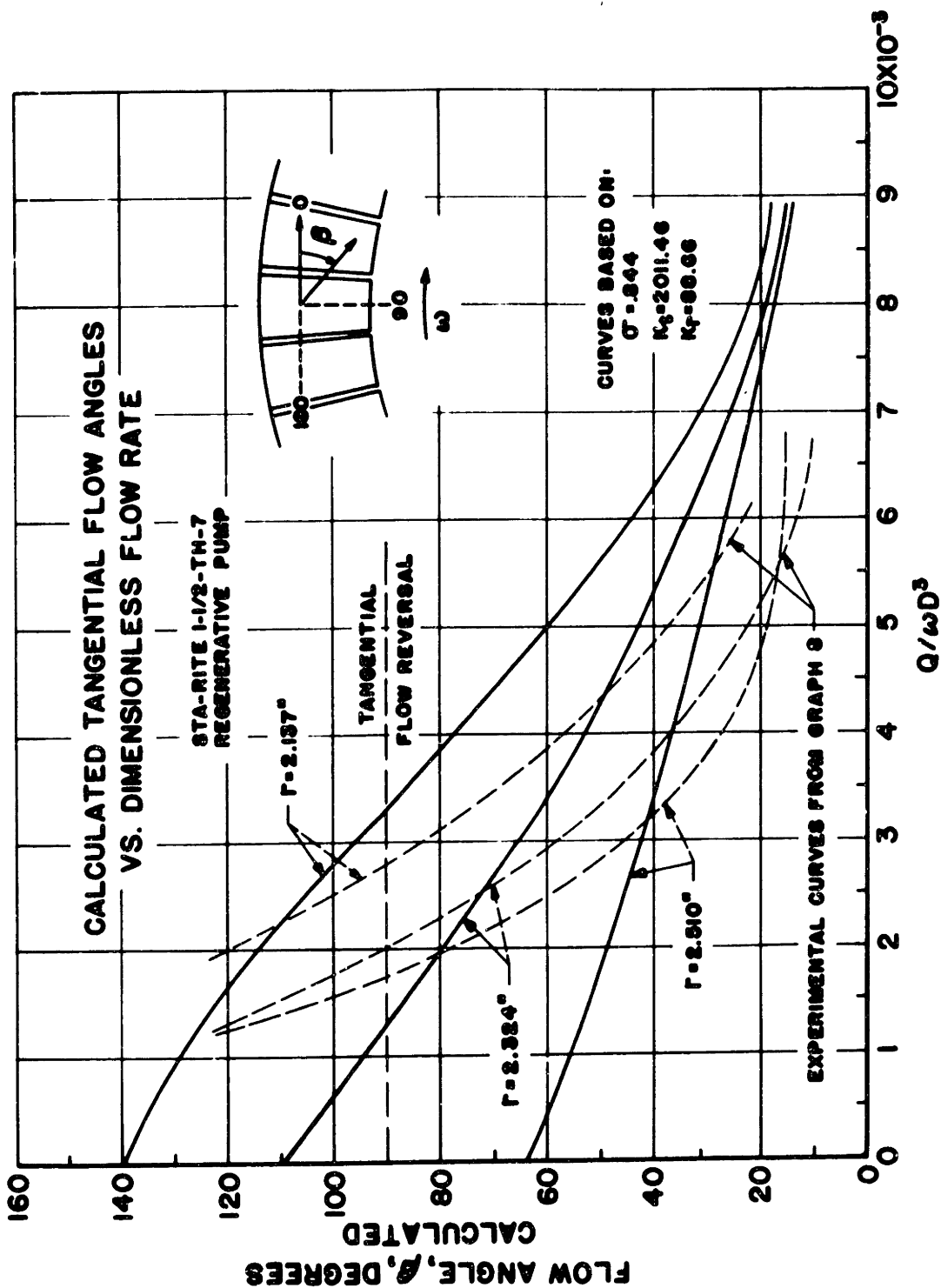
**GRAPH 6**

THEORETICAL POWER DISTRIBUTION AT 3600 RPM OF REGENERATIVE PUMP.

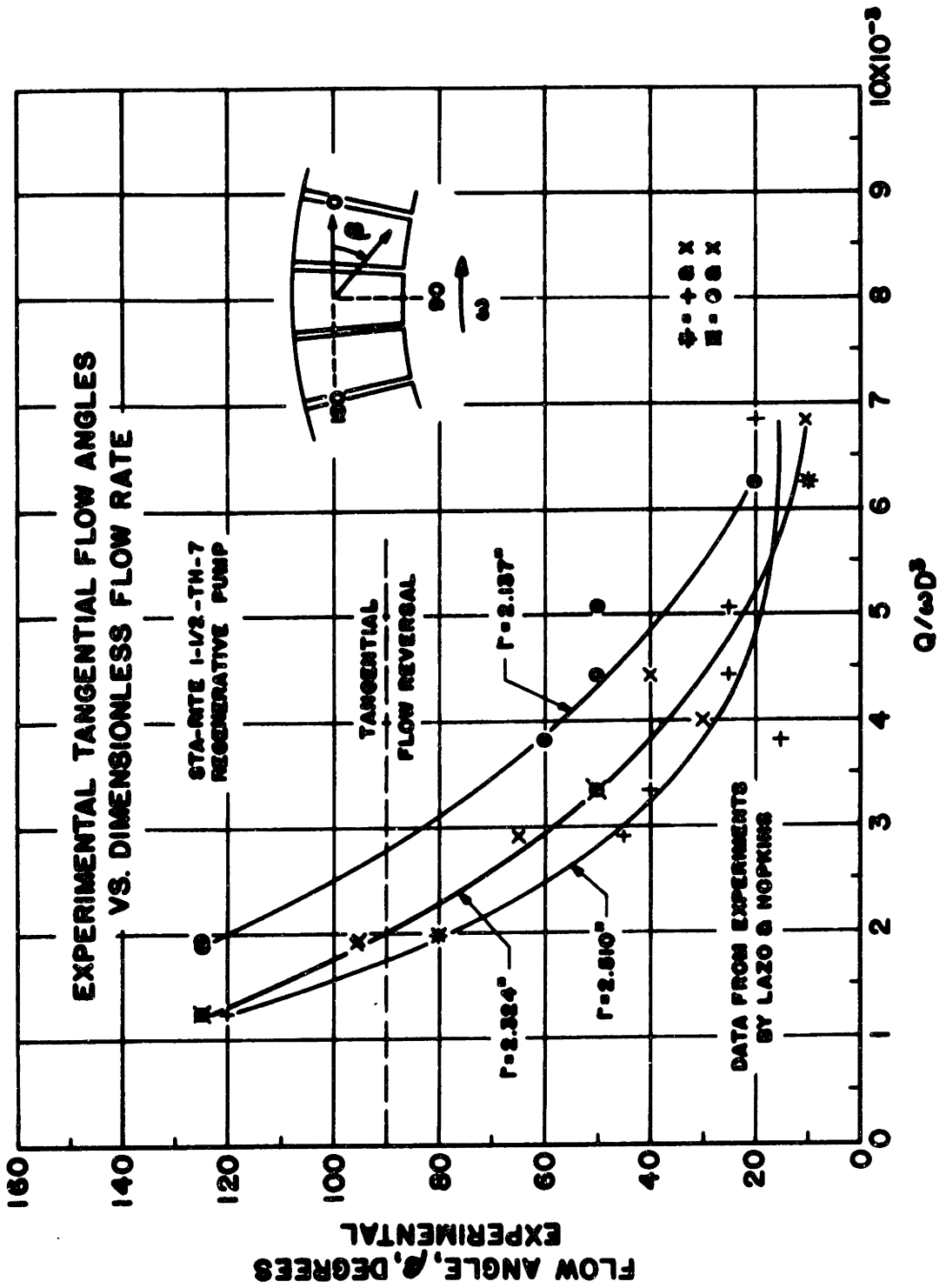
As shown, the blade entrance loss is the greatest consumer of power over most of the range of operation, and its decrease would reduce power input and increase head most effectively. This loss might be reduced somewhat by rounding the radial edges of the vanes, particularly the back edge. However, without guide-vanes in the now open channel, substantial decrease of the blade entrance loss cannot be expected. The gain, if any, would be over a very limited range of operation.

Most of the tangential losses, from the theory in the analysis, are due to irreversibilities in the inlet and discharge rather than in the working section of the pump. Their reduction, therefore, is dependent mainly on improved design of the inlet and discharge--not on improved internal performance. From this discussion we conclude that the most feasible method of improving performance is the reduction of the radial losses.

Because of the two-dimensional treatment in the analysis, with its approximations and assumptions, it cannot fully and accurately predict all internal mechanics of the true three-dimensional flow. To be valid it must nevertheless qualitatively agree with the internal flow pattern. Perhaps the most significant mechanism of the flow is the reversal of the tangential velocity near the blade root as shut off is approached. This is represented in the theory by the negative values of  $\alpha$ , as shown in



**GRAPH 7**  
**CALCULATED TANGENTIAL FLOW ANGLES.**



**GRAPH 8**  
**EXPERIMENTAL TANGENTIAL FLOW ANGLES.**

Graph 5. The tangential flow angles in the open channel at the side of the rotor were measured at various radii and flows by Lazo and Hopkins. Graph 7, page 70, shows very satisfactory qualitative agreement between the three-dimensional data of the experimental curves and the curves calculated from the two-dimensional theoretical solution. Unfortunately, because of the construction of the test pump, it was necessary to read these angles by looking into a forty-five degree mirror set in a specially machined recess. The resulting experimental scatter, even after collecting the data on a dimensionless plot, is evident in Graph 8, page 71.

## XV. SUMMATION

The analysis developed in this paper for a regenerative pump is more complete than that of other turbomachinery. Generally, the theory of centrifugal pumps, turbines, axial-flow compressors, and other hydrodynamic units, is best suited to the maximum efficiency point and uses quite a number of empirical constants determined by experience. The theory we have proposed has been verified over the complete range of operation. Only three constants, each independent of capacity and uninfluenced by speed or fluid medium, were introduced.

Of course, the analysis has weaknesses due to the assumptions and approximations necessary. One of the



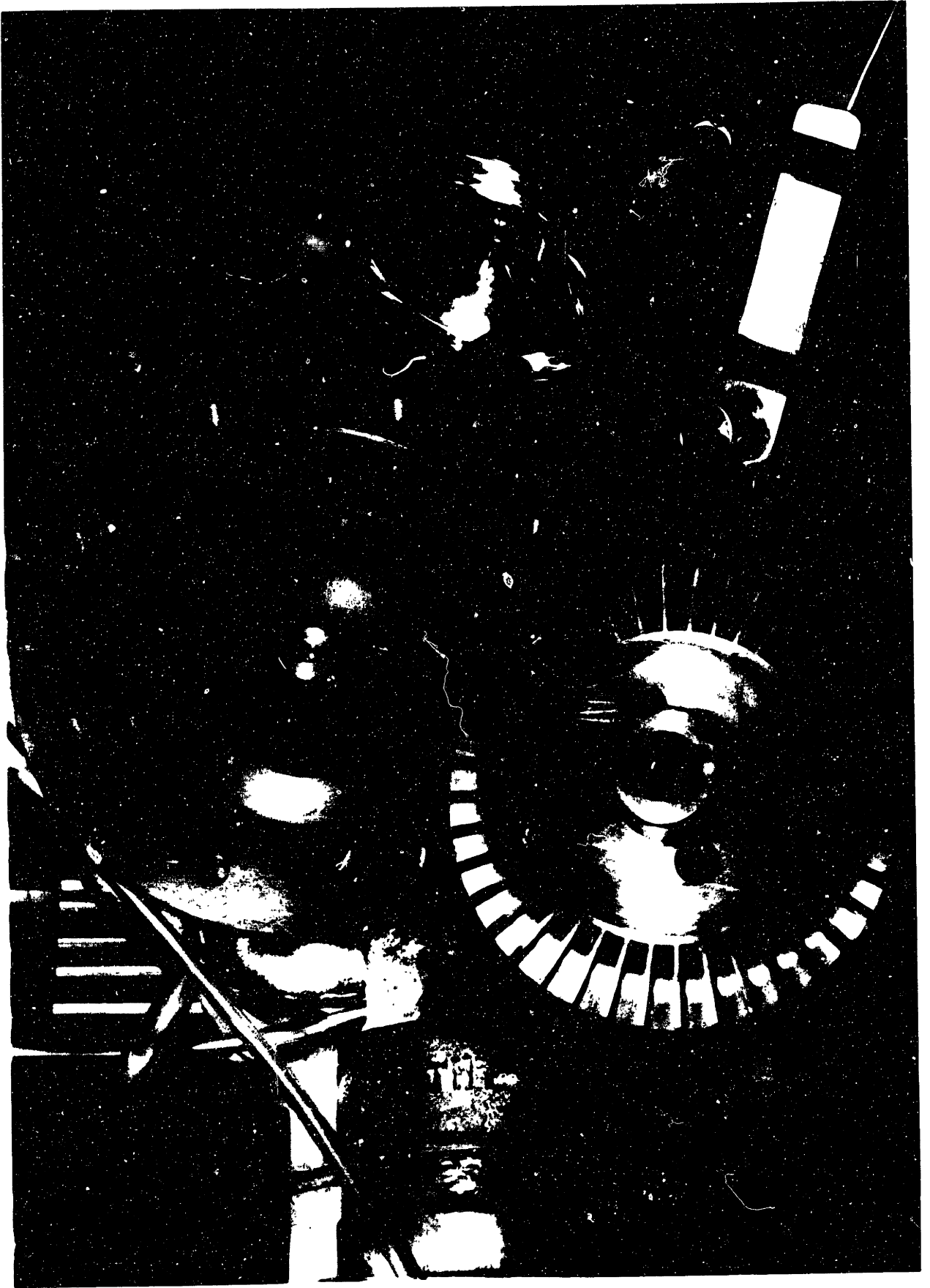
weaknesses is that while variation in the experimental data collected will only slightly alter the resulting experimental curves, a reasonable change in any one of the data points used in determining the constants causes a significant change in the resulting theoretical curves. This means that to predict the operation of a unit over its complete range the three constants must be pre-evaluated quite accurately. From a practical point of view, future study might be best directed toward prediction of the maximum efficiency point. My next plan is to study this phase of the overall project.

Two forms of losses were not considered in the solution--mechanical friction and internal leakage. All losses due to mechanical friction, except disk-friction losses, were eliminated from the experiments by the nature of the test set-up. The disk-friction losses, on a percentage basis, are very small and would alter the efficiency curve less than consideration of experimental error. Internal leakage through the side clearances and through the stripper apparently has a very noticeable effect. In the experiments by Lazo and Hopkins the sum of the side clearances was 0.003 to 0.005 inches. The clearance was opened to a total of 0.012 inches in later experiments, and it was found that the similitude characteristics were significantly altered. The real effect of internal leakage is yet to be studied.

The analysis certainly satisfies our primary objective. Now that the governing equations are determined, the problems of pre-evaluating the "coefficient of slip" and the radial and tangential loss coefficients, and improving performance, can be studied. Many experimental problems were encountered in using a test model built for the commercial market. On several occasions, experiments were not feasible because of the small dimensions of the unit, as shown by the list in the appendix, or because of the design. To offset this handicap, and at the same time give versatility and greater visibility, a specially designed plastic model is now in production. This model, which is actually a "half-pump," is a  $3\frac{1}{2}$  to 1 scale version of the present test unit. The increased dimensions may allow the use of probes in the fluid stream, which was not possible before, and will increase the accuracy in measuring flow angles. Just as important is the new model's versatility. It has been designed so that axial and radial dimensional changes can be made and blades of various design can be used in the rotor. It is anticipated that experimental results from this unit, in conjunction with the theory, will lead to a greater understanding of the influence of dimensional changes. The findings of this phase of the project will be reported in a thesis by Miguel A. Santalo.

APPENDIX

<u>Contents</u>	Page
Photograph of Rotor and Internal View of Test Pump . . . . .	76
Dimensions of Sta-Rite 1 $\frac{1}{2}$ -TH-7 Regenerative Pump. .	77
Derivation of Tangential Velocity Equation with Friction Introduced in Equations of Motion . .	78



DIMENSIONS OF THE STA-RITE 1 $\frac{1}{2}$ -TH-7 REGENERATIVE PUMP:

$r_1$	. . . . .	1.952 in.
$r_2$	. . . . .	2.697 in.
$r_3$	. . . . .	2.787 in.
$b$	. . . . .	0.2295 in.
$c$	. . . . .	0.1810 in.
$d$	. . . . .	0.3080 in.
$L$	. . . . .	0.2688 in.
$l$	. . . . .	0.1540 in.
$r_{cg}$	. . . . .	2.392 in.
$A_1$	. . . . .	0.02066 in <sup>2</sup>
$A_2$	. . . . .	0.04865 in <sup>2</sup>
$A_3$	. . . . .	0.25718 in <sup>2</sup>
$A_4$	. . . . .	0.03534 in <sup>2</sup>

DERIVATION OF TANGENTIAL VELOCITY EQUATION WITH  
FRICTION INTRODUCED IN EQUATIONS OF MOTION

Shear forces are experienced at all surfaces of a control volume of a viscous fluid where a velocity gradient exists. For simplification, however, we follow the generally accepted practice of assuming all shear effects act as a single force at the solid boundaries. Even with this simplification, taking the true components of the shear force acting in the absolute direction of the flow leads to differential equations out of the scope of most engineering mathematical texts. We further simplify by assuming the shear forces are of the form -

$$\begin{aligned} \text{Tangential shear force} &= \rho f_t \frac{v_u^2}{2g} r d\theta dr \\ \text{Radial shear force} &= \rho f_r \frac{v_r^2}{2g} r d\theta dr \end{aligned}$$

We select for this example the control volume between points 2 and 3 on page 18. Each of the shear forces above, of course, is assumed acting against fluid motion. The new differential equations of motion, derived as before, are now:

In the tangential direction,

$$(1) \quad \frac{\partial v_u}{\partial r} + \frac{v_u}{r} + \frac{f_t}{2Q_c} v_u^2 r = - \frac{b}{\rho Q_c} \frac{\partial p}{\partial \theta}$$

In the radial direction,

$$(2) \quad \frac{\partial p}{\partial r} = \rho \frac{v_u^2}{r} + \frac{\rho Q_c^2}{b^2 r^3} \left( 1 - \frac{f_r}{2b} r \right)$$

These equations are non-linear first-order functions of the form of Riccati's Equation:<sup>1</sup>

$$(3) \quad \frac{dy}{dx} + P(x)y + Q(x)y^2 = R(x)$$

where  $P(x)$ ,  $Q(x)$ , and  $R(x)$  are functions of the independent variable. Equations of this form can be solved by the substitution,

$$(4) \quad Y = \frac{1}{Q(x)} u \quad \frac{du}{dx}$$

which reduces Riccati's Equation to a linear second-order relation.

$$(5) \quad \frac{d^2u}{dx^2} + \left[ P(x) - \frac{1}{Q(x)} \frac{dQ(x)}{dx} \right] \frac{du}{dx} - R(x)Q(x)u = 0$$

Since we are interested in the equation for the tangential velocity, in equation (1) let,

$$k_1 = \frac{f_t}{2Q_c}$$

and,

$$k_2 = \frac{b}{\rho Q_c} \frac{dp}{d\theta}$$

Using  $r$  as the independent variable:

$$P(r) = \frac{1}{r}; \quad Q(r) = k_1 r; \quad \text{and} \quad R(r) = -k_2$$

Equation (5) becomes,

$$(6) \quad \frac{d^2u}{dr^2} + k_1 k_2 r u = 0$$

---

<sup>1</sup> See problem 34, page 56, of Advanced Calculus for Engineers by F. B. Hildebrand. Prentice-Hall, New York, 1949.

The simplest solution of this equation is found using Bessel functions,  $J$ , and is,

$$(7) \quad u = r^{\frac{1}{2}} \left[ C_1 J_{\frac{1}{2}} \left( \frac{2\lambda}{3} r^{\frac{3}{2}} \right) + C_2 J_{-\frac{1}{2}} \left( \frac{2\lambda}{3} r^{\frac{3}{2}} \right) \right]$$

where  $\lambda = \sqrt{k_1 k_2}$ , and  $C_1$  and  $C_2$  are arbitrary constants.

Comparison of the equations (1) and (3) shows that,

$$(8) \quad V_u = y = \frac{1}{Q(r) u} \frac{du}{dr}$$

Substituting in equation (8) after the indicated operations, and simplifying,

$$(9) \quad V_u = K_1 r^{-\frac{1}{2}} \left[ \frac{J_{-\frac{1}{2}}(K_2 r^{\frac{3}{2}}) - C J_{\frac{1}{2}}(K_2 r^{\frac{3}{2}})}{J_{\frac{1}{2}}(K_2 r^{\frac{3}{2}}) - C J_{-\frac{1}{2}}(K_2 r^{\frac{3}{2}})} \right]$$

where now,

$C =$  arbitrary constant

$$K_1 = \sqrt{\frac{\partial p}{\partial \theta} \frac{2b}{\rho f_t}}$$

and,

$$K_2 = \frac{2}{3Q_c} \sqrt{\frac{\partial p}{\partial \theta} \frac{b f_t}{2\rho}}$$

To carry on the analysis, it would first be necessary to determine the arbitrary constant from a known boundary condition. In solving the differential relation of equation (2), the square of equation (9) would be substituted for  $V_u^2$  before integrating. As stated in the text, the mathematical complication of this attack is unwarranted in the light of the original assumptions.



BIBLIOGRAPHY

- Senoo, Yasutashi, "Theoretical Research on Friction Pump," Reports of the Research Institute for Fluid Engineering, Vol. 5, No. 1, Japan, 1948.
- Wilson, Warren E., "Analysis of Turbine Pumps," Product Engineering, October, 1947.
- Mizadzu, A., "Theory of Wesco Rotary Pump," Transactions of the Society of Mechanical Engineers of Japan, Vol. 15, No. 18, February, 1939.
- Lippman, D., and Taylor, T., "Design and Construction of Test Equipment for a Regenerative Fluid Pump," Senior Thesis, Massachusetts Institute of Technology, January, 1953.
- Lazo, L., and Hopkins, T., "Theoretical and Experimental Analysis of a Regenerative Turbine Pump," Senior Thesis, Massachusetts Institute of Technology, January, 1953.
- Lutz, Gilbert F., "Experimental Investigation of the Pressure Distribution in a Regenerative Turbine Pump, the Sta-Rite TH-7," Senior Thesis, Massachusetts Institute of Technology, May, 1953.
- Wislicenus, George F., Fluid Mechanics of Turbomachinery, McGraw-Hill, New York, 1947.
- Hunsaker and Rightmire, Engineering Applications of Fluid Mechanics, McGraw-Hill, New York, 1947.
- Hildebrand, F. B., Advanced Calculus for Engineers, Prentice-Hall, New York, 1949.